

# EEG Right & Left Voluntary Hand Movement-based Virtual Brain-Computer Interfacing Keyboard with Machine Learning and a Hybrid Bi-Directional LSTM-GRU Model

*Biplov Paneru<sup>1</sup>, Bishwash Paneru<sup>2</sup>, Sanjog Chhetri Sapkota<sup>3</sup>*

*<sup>1</sup>Department of Electronics and Communication Engineering, Nepal Engineering College, Affiliated to Pokhara University, Bhaktapur, Nepal*

*<sup>2</sup>Department of Applied Sciences and Chemical Engineering, Institute of Engineering Pulchowk Campus, Affiliated to Tribhuvan University, Lalitpur, Nepal*

*<sup>3</sup>Nepal Research and Collaboration Center, Nepal*

*Corresponding author email: biplovp019402@nec.edu.np*

## **Abstract**

Significant advancements have been achieved in Brain-Machine Interface (BMI), particularly in electroencephalography (EEG)-based systems, which capture the brain's electrical activity dynamics non-invasively. This study focuses on EEG-based BMI for detecting voluntary keystrokes, aiming to develop a reliable brain-computer interface (BCI) to simulate and anticipate keystrokes, especially for individuals with motor impairments. The dataset, featured in a Nature publication, was initially band-pass filtered and segmented into 22-electrode arrays, and our work began with excluding non-significant channels (A1, A2, and X5), and the feature-extracted dataset was utilized for developing models. Using ERP window-based segmentation, each window was categorized relative to Event 0, resulting in a 19\*200 data array of features set. The ERP window-based data segmentation was done with those below Event 0 belonging to one and above Event 0 belonging to another window so that total electrode data division resulted in a total of 19\*200 data arrays to begin model development. The methodology includes extensive segmentation, event alignment, ERP plot analysis, and signal analysis. Different deep learning models are trained to classify EEG data into three categories—'resting state' (0), 'd' key press (1), and 'l' key press (2). Real-time keypress simulation based on neural activity is enabled through integration with a tkinter-based graphical user interface. Feature engineering utilized ERP windows, and the SVC model achieved 90.42% accuracy in event classification. Additionally, deep learning models—MLP (89% accuracy), Catboost (87.39% accuracy), KNN (72.59%), Gaussian Naive Bayes (79.21%), Logistic Regression (90.81% accuracy), and a novel Bi-Directional LSTM-GRU hybrid model (89% accuracy)—were developed for BCI keyboard simulation. Finally, a GUI was created to predict and simulate keystrokes using the trained MLP model.

**Keywords:** *EEG, Brain Computer Interface, tkinter, Bi-Directional -LSTM-GRU, Hyperparameters, ERP, Movement onset*

## INTRODUCTION

Thus far, new prospects for the research of neurodegenerative diseases have been brought about by enhanced neuroimaging techniques that enable the non-invasive investigation of the structural and functional structure of the brain [16]. A non-invasive neuroimaging method called electroencephalography (EEG) records and quantifies the electrical activity produced by brain neurons. It entails applying electrodes to the scalp in order to record the electrical impulses generated when neurons fire. With its high temporal resolution and real-time view of brain activity, EEG can shed light on neurological disorders, emotions, and cognitive processes. This method is extensively employed in neuroscience research, clinical settings, and the growing field of brain-computer interfaces (BCIs) for a variety of uses, such as assistive technologies for people with motor neuron disorder. Technologies known as brain-computer interfaces (BCIs) are designed to create a link between the human brain and other electronic systems. The potential of BCI technology has been shown by earlier studies employing non-invasive BCI to operate real-world things like wheelchairs and quadcopters as well as virtual objects like computer cursors and virtual quadcopters [25]. Neural information can be obtained from electroencephalograms (EEGs), which are non-invasive methods of recording brain electrical activity. Artificial intelligence (AI) applications, such as sophisticated signal processing and machine learning algorithms, interpret EEG data to interpret user intent and enable control over external devices. These technologies could be brain-computer interfaces (BCIs), which provide a lifeline to people struggling with motor neuron disorders by interpreting EEG signals to operate wheelchairs, prosthetic limbs, or other assistive devices. The human brain and computer can now communicate through a new channel thanks to brain computer interfaces, or BCIs [1]. The development of brain-computer interface (BCI) technology has changed how people interact as shown in figure 1. with computers and created new opportunities for studying and harnessing the power of the human brain [17]. The development of new technology has made machines an indispensable aspect of modern life. There are numerous ways a healthy individual might engage with these devices. These interactions frequently need for deft manipulation of body parts (e.g., hand, head, finger) [12].



**Fig 1.** Brain Computer Interfacing illustration

People must communicate. Communication needs continue to be one of the key problems for those who have locked-in syndrome (LIS). Although there are a lot of commercially available assistive and augmentative communication systems that use different physiological signals, the demand is not fully satisfied. When current choices are insufficient, brain interfaces—in particular, those that use event related potentials (ERP) in electroencephalography (EEG) to noninvasively detect a person's intent—are emerging as a possible communication interface to satisfy this

need [2]. With this research study we want to innovate a new solution that uses brain signals to control a virtual keyboard, making computer interfaces more inclusive and accessible with help of SVM and MLP, EEGNet, and novel hybrid neural network algorithm with successive testing. We plan to do this by utilizing BCI technology along with AI models. Though research on brain-computer interfaces (BCI) has advanced quickly, putting BCI systems to use in daily life is still a difficult task. Current virtual keyboards are frequently inflexible and unable to meet the needs of a wide range of users, particularly those with impaired motor control. The lack of effective and user-friendly virtual keyboards based on BCIs restricts the use of digital platforms by people with motor disabilities. Also, the first ever deep learning based approach for development of BCI keyboard as well as first step for right-left hand voluntary hand movement based virtual keyboard control using AI model this work has a great contribution. By creating a reliable BCI system that is integrated with a virtual keyboard, this project seeks to close these gaps, addressing the unique difficulties faced by people who have motor impairments and expanding the boundaries of human-computer interaction. Technical artifacts such as electric power source noise and amplitude artifacts, as well as biological artifacts including ocular artifacts, ECG and EMG artifacts, are present in the Electroencephalogram (EEG) data. One of the primary artifacts in the EEG data is the blink of the eye. However, in this case, eye blinks are control signals that are used to choose the blocks and characters in the virtual keyboard rather than being artifacts. The control signals are identified by utilizing the kurtosis coefficient and amplitude properties of the eye blink signals [1].

Peer-to-peer communication relies heavily on speed as well; a message that is not delivered on time frequently loses significance. Therefore, to aid letter selection during brain-typing, we employ rapid serial visual presentation (RSVP) in combination with language models. Our ultimate goal is to create a system that simultaneously attains great accuracy and speed. This report shows preliminary findings from the currently under construction RSVP Keyboard system. These first findings on healthy, locked-in people suggest that the RSVP Keyboard paradigm may enable accurate letter selection in a single trial or a few trials [2].

A poll was conducted to highlight the design methods used in the existing EEG-EOG virtual keyboard. We wrapped up by talking about the possible benefits of integrating the two systems and offering suggestions to provide in-depth understanding for any future design problems pertaining to EEG-EOG BCI systems. Lastly, a novel EEG-EOG BCI system's overall architecture was suggested. The traditional view of the eye movement features in the EEG signals artifacts that need to be eliminated is completely changed by the proposed hybrid system; instead, EOG traces are extracted from the EEG in our proposed hybrid architecture and are treated as an extra input modality sharing control in accordance with the selected design protocol [3].

The game also incorporates a number of standard control techniques found in commercial games, such as keyboard keystrokes. Based on the sample entropy features and band power values in the alpha, beta, and theta bands of the EEG, three distinct degrees of attention have been identified in the players. Using keyboard and EEG-based controls, three subjects have successfully traversed the specified 3-D environment. According to experimental findings, it is possible to combine traditional control inputs with brain signal-based inputs in multi-player neurofeedback games to enhance brain function [4].

These two methods work together to provide BCI that is based on EEG. In this research, we use EEG to develop four states BCI for a neurodegenerative patient by analyzing the signal for four mentally composed tasks utilizing band power and radial basis function. An analysis of the wheelchair's performance for a person with neurological disease was done online. The outcome demonstrates that the four tasks were completed with an average classification accuracy of 92.50% overall and 95%, 87.50%, 92.50%, and 95.00% for each individual task. The outcome demonstrates the ability of control directives derived from the EEG signal to operate intelligent devices [5].

Two severely disabled volunteers maneuvered a power wheelchair using the sensing platform as a research case. The participants completed 15 typical wheelchair-user tasks, and a standard test was used to assess their abilities. For volunteers A and B, they used the head control to get 93.3 and 86.6%, respectively; for the voice control, they got 63.3 and 66.6%, respectively. These findings demonstrate that end users were able to execute at a high level by utilizing the head movements interface to build the majority of their skills [7].

A biosensor is used in a BCI system to record EEG and MPG signals. The ThinkGear MATLAB module will process the signals. To control the wheelchair, the Level Analyzer Technique is applied to all training signals, extracting the Alpha and Beta waves. Over radio frequency (RF) technology, the command signals are sent to the microprocessor. The ARM 7 microprocessor in the robotic module is connected to a DC motor to carry out the command. The

wheelchair's direction was adjusted based on the user's level of concentration and eye blinking intensity. If the wireless BCI system is improved, wearable, and portable, paraplegic people may be able to operate their wheelchairs with ease [8].

Shutting their eyes 15 ALS patients had their EEGs recorded, and the spectral band power was computed in the following frequency bands: delta-theta band (1-7 Hz); low alpha (IAF - 2 Hz - IAF); high alpha (IAF - IAF + 2 Hz); and beta (13 - 25 Hz). These bands were established based on individual alpha frequency (IAF). The duration, incidence, and coverage of EEG microstate measures were also assessed. A number of clinical ratings measuring impairments and the course of the disease were associated with spectral band powers and microstate parameters. Fifteen healthy participants were recruited as a control group [11].

This work presents the construction of a revolutionary hybrid speller/keyboard system that integrates steady state visual evoked potential (SSVEP) and electro-oculogram (EOG). The traditional EOG-based speller system has a cap on the total number of targets it can select and requires continual eye movements to select a single target. Nine groups of 36 targets—alphabets, digits, and special characters—are included in this suggested speller. There are two phases to target selection. The target groups are chosen using a variety of eye motions (winks, blinks, and gazes), and the target is then identified using SSVEP. The information transmission rate (ITR) of the proposed system is 70.99 ( $\pm 9.95$ ) bits/min, and its average classification accuracy is 94.16% [12].

The invention presents a sort of multi-mode EEG signals dummy keyboard design method. This method uses the event related potential (ERP), a type of specific brain evoked potential that reflects variations in the electrophysiology of the deuterocerebrum, which is the cognitive process. The term SSVEP refers to the brain's periodic modulation of a specific frequency (more than 6 Hz) in response to external stimuli. SSVEP can be detected using Canonical Correlation Analysis (CCA), which can extract spectrum signatures of 12 Hz, 15 Hz, and 18 Hz. As a result, ERP early stage ingredients N1, P2 can significantly increase the accuracy rate of the dummy keyboard based on EEG signals as the keyboard's row coordinate and the corresponding spectrum signatures of SSVEP as the keyboard's row coordinate [13].

This study aims to provide an EEG brain-computer interface (BCI), bionics, and Emotiv system through smart phone application for basic communication as a treatment for ALS patients. Its goal is to enable ALS sufferers to have more control over their surroundings and to interact through a computer interface with their loved ones or caregivers [14].

This work describes a control tool that forms a braincomputer interface (BCI) by receiving system signals from the frontal lobe. The control tool uses the Neurosky Mindwave headset, which detects brainwaves (voluntary blinks and attention). In place of the traditional computer input mechanism, this study suggested an alternate one for physically challenged disabled individuals. The study recommended using two virtual keyboard layouts. An important finding in the experiment's development of user printing proficiency on PCs was made. In comparison to previous studies, encouraging results (1.55–1.8 WPM) were obtained in this one [15].

A brain-signal analysis BCI system identifies users and grants them autonomy. People who are handicapped or disabled can simply roll their wheelchair in any direction because to this technology. The primary reason for utilizing this sensor is its portability and ease of use; in contrast, older EEG sensors are bulkier and require more time to begin collecting data; therefore, the Neurosky sensor is more advantageous than the older EEG sensor. This prototype idea uses Neurosky sensor or EEG technology to interface the brain with a wheelchair [18].

Modern EEG-based BCI applications, especially those that use motor-imagery (MI) data, are presented in this systematic review with regard to wheelchair control and mobility. It provides a comprehensive overview of the many research carried out since 2010, with an emphasis on the approaches employed for algorithm analysis, features extraction, features selection, and classification, as well as wheelchair components and performance assessment. The findings presented in this work have the potential to draw attention to novel research areas and draw attention to the shortcomings of the biological instruments currently used to treat individuals with severe disabilities [19].

The authors of this work suggest a revolutionary triple RSVP speller that has greater ITR and gaze- and space-independent properties. The triple RSVP speller achieved an average online accuracy of 0.790 and an average online

ITR of 20.259 bit/min, according to the experiment results. The system spelled at a pace of 10 s per character, with a  $90 \times 195$  pixel rectangle serving as the stimulus presentation interface. Thus, mobile smart devices (smart watches, cellphones, and other devices) can incorporate the triple RSVP speller [20].

In this study, the authors discovered that using a combination of two sequential low-dimensional controls, a group of thirteen human participants could voluntarily modify brain activity to control a robotic arm with good accuracy for tasks requiring numerous degrees of freedom. In just a few training sessions, the subjects were able to modulate their brain rhythms to effectively control the robotic arm's reaching, and they were able to sustain this control across several months. The outcomes show that non-invasive BCI technology can be used to operate prosthetic limbs by humans [21].

The method involves using a model built on the ibug 300-W dataset to teach the machine to recognize keypress events and blinks. The system's effectiveness in real-time communication is demonstrated by the results of extensive testing, which include accurate blink recognition, user-triggered actions using Flask, and timely caregiver alerts through WhatsApp. This method offers possibilities for more general assistive technologies aimed at improving the quality of life and communication for those with motor function deficits, and it has applications beyond ALS. By offering practical answers, the research enhances healthcare technology and raises the standard of living for those suffering from neurodegenerative disorders [22].

This study describes the creation of an EEG-based brain-controlled wheelchair using Brain Computer Interface (BCI) and a NeuroSky Mind Wave EEG headset. Patients who are quadriplegic are unable to move any body organs below their necks. By using this technology, people who are quadriplegic will be able to move around independently. The patient's fluctuating attention level regulates the wheelchair's movement. The patient can blink their eyes twice to turn on or off this device. The wheelchair's design incorporates a fuzzy image based on graphics to let patients adjust their level of concentration as needed [23].

The design and development of a robotic vision system that is controlled by an interactive Graphical User Interface (GUI) application are presented in this study. This rationale led to the system's architecture, which enables a novice user to utilize the gadget with minimal guidance. Through the program, users can specify what they want to be picked up and placed by a robotic arm in the desired spot. Users of the application can filter things according to their size, color, and shape. After that, the arm moves through a series of predetermined locations to pick up the object, place it, and finally move back to the starting position. A microcontroller receives the joint coordinates and uses them to determine the arm's joint angle at each place [24].

By combining two sequential low-dimensional controls, the researchers in this study discovered that a group of thirteen human participants could voluntarily modify brain activity to control a robotic arm with great precision for tasks requiring numerous degrees of freedom. Through brain rhythm modulation, subjects were able to efficiently control reaching of the robotic arm in a matter of only a few training sessions, and they were able to sustain this skill over several months. The outcomes show that non-invasive BCI technology can successfully enable human operation of prosthetic limbs [25].

This paper describes our experiences in building a virtual keyboard implemented using a Brain-Computer Interface (BCI) that interacts with the eMotiv EPOC Neural Headset. The contribution of the work is an alternative input device for those who have a motor disability and are challenged by traditional input devices. The advantages of a virtual keyboard based on BCI are summarized and we describe its design and implementation. We also present the results of a preliminary study that has suggested several improvements for enhancing the effectiveness of the virtual keyboard [26].

The goal of this project is to create a virtual keyboard based on a Brain Computer Interface (BCI) that can be operated by the brain's bioelectrical signals. With 36 keys overall, the virtual keyboard is built in accordance with "QWERTY" specifications. Two modules comprise the research: the hardware module and the software module. Red, green, and blue (RGB) color analysis of the EEG signals is done in the Software module via an asynchronous technique. Two sessions of the study were held with university students. The findings revealed an average spelling completion time of 2.3 minutes and an accuracy of 89.7% with 6.4 characters per minute (CPM). People with neuromuscular diseases, such as paralysis from cerebral palsy, spinal cord injury, or stroke, have found success with the virtual keyboard [27].

Using bioelectrical waves from the human brain, a BCI base virtual keyboard with 36 keys total—26 English alphabets from A to Z, 7 special characters, and 3 action keys—was built in this study in accordance with "QWERTY" standards. Two modules comprise the research: a software module and a hardware module. Red, green, and blue (RGB) hues are detected in electroencephalogram (EEG) signals via an asynchronous process. Following an experiment conducted on the same subjects (university students) over two sessions, the results are concluded. The experiment's findings show an average accuracy of 89.7%, a speed of 6.4 characters per minute (CPM), and an average spelling completion time of 2.3 minutes [28].

This work proposes the virtual keyboard (VK), an asynchronously controlled three-class brain-computer interface-based spelling device that is regulated by motor imagery and driven by spontaneous electroencephalogram. Two of the three physically fit participants that used the VK successfully achieved the first results, which showed an increase in the spelling rate ( $\text{/spl } \sigma\text{/}$ ) and the quantity of correctly spelled letters ( $\text{/min}$ ) up to  $\text{/spl } \sigma\text{/} = 3.38$  (average  $\text{/spl } \sigma\text{/} = 1.99$ ) [29].

In order to help patients with Locked-In syndrome or ALS, this work presents a novel LabVIEW based algorithm for the creation of an eye-blink strength controlled virtual keyboard-based brain-computer interface. The virtual keyboard built with LabVIEW offers the following functions: it can detect and count the voluntary eye blinks; it can switch between commands and select commands; it can highlight actions that are happening concurrently with the previously mentioned processes; and it can enable cancel, delete, and space commands. The Divide and Conquer concept serves as the foundation for the suggested virtual keyboard's operation. As a result, choosing a row, half row, or key related to the character that needs to be introduced in the text box may involve flipping between the rows, half rows, and keys (characters) [30].

Much research gap lies on EEG based keyboard development, and Machine learning implementation is very rare in the context of neuro keyboard development so we aim to introduce first ever EEG-based virtual keyboard in deep learning along with simulating keypress using new person EEG data. For keyboard development with SVM has been utilized in [28] which is only research work utilizing machine learning techniques for such research work. This research work is also important as the Right-Left hand voluntary movement-based EEG assistive technologies hasn't been implemented before so, we aim to fulfill this big research gap by developing a deep learning model powered virtual keyboard for predicting human brain signals of 19 electrodes and predicting keypress of buttons 'd' and 'l'.

## **Objectives and scope**

The creation of a system that can serve as an interface to connect the human brain to the control system is known as a brain-computer interface. The development of a GUI-based virtual keyboard as an assistive technology for

individuals with neurogenerative disabilities such as ALS and other motor neuron diseases is the exclusive goal of our project's Brain Computer Interfacing project.

The main objectives of this project are:

- i. To develop an EEG-based virtual keyboard system.
- ii. To train Machine Learning models for time series EEG data to predict keypress events.
- iii. To simulate keypress actions with a tkinter-based GUI application based on the trained model.

### Applications

The BCI-Based Virtual Keyboard project has a wide range of applications that could have a big impact on human-computer interaction and assistive technology. The system primarily provides an alternate form of communication, making it an invaluable assistive tool for people with neurodegenerative diseases like ALS and motor neuron disorders. The applications of the project are:

- i) Assistive technology for people with neurogenerative diseases and motor neuron affected victims.
- ii) The project can be implemented for developing applications that can be useful for Brain Computer Interfacing systems development.

### METHODOLOGY

The dataset used in this work is based on the FreeForm paradigm from the Nature paper [6], which focuses on the EEG signal-based discrimination of voluntary motor movements. The subjects interacted with an eGUI that allowed for FreeForm interaction, focusing on a fixation point and freely pressing the "d" or "l" keys with their left or right hand at random intervals. The neural activity changes that preceded key presses were captured by the EEG signals, which served as the foundation for further analysis.

The dataset is divided into three sets: Recording session of subject C: FREEFORM-SubjectC-151210-5St-LRHand.mat., similarly, FREEFORMSubjectB1511112StLRHand.mat, and also FREEFORMSubjectC1512102StLRHand are three sets of data obtained from recording sessions in the experiment. FreeForm—the identification of voluntary left- and right-hand movements—is the recording session paradigm. There are two states of mental imagery (2St). The Left-Right Hand (LRHand) mnemonic is used during recording sessions is shown in table 1.

**Table 1.** Onsets in the EEG dataset

S.no.	Dataset	No.of Keystroke events
1.	FREEFORMSubjectC1512082StLRHand	688
2.	FREEFORMSubjectB1511112StLRHand.mat	739
3.	FREEFORMSubjectC1512102StLRHand	700

The total number of user keystroke events during the activity that correspond to the stimuli or event during keypress or resting state is referred to as the onsets in the EEG recording in table 1. A crucial component of the classification problem is the onsets information that was acquired.

Each record in the dataset is distinguished by a unique alphanumeric identifier referred to as "id." This identifier serves as a key element for record tracking and management. The "nS" parameter denotes the number of EEG data samples contained within each record, providing insight into the temporal dimension of the recorded neural signals. The "sampFreq" parameter specifies the sampling frequency of the EEG data, representing the rate at which data points are collected per unit of time. The "marker" field encapsulates the eGUI interaction record of the recording session, offering contextual information about user actions during the EEG data acquisition [6]. Finally, the "data" field encapsulates the raw EEG data for the respective recording session, serving as the primary source for subsequent preprocessing, feature extraction, and model training in the context of the BCI-Based Virtual Keyboard.

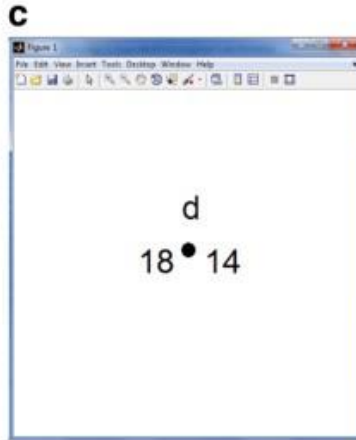


**Figure 2. FreeForm-interaction eGUI screen [6]**

During the preprocessing stage, trials are extracted from the 200 Hz EEG data sample and aligned with the key press events that were recorded. Event plots with markers are used to identify and visualize these events. ERP (Event-Related Potentials) plots and other additional analysis techniques are used to improve the signal quality and discriminate neural patterns. If the ERP results are not conclusive, more techniques such as filtering are investigated to improve the data quality.

A deep learning model is trained for classification after preprocessing. The eGUI's "0" label denotes a resting stage, "1" denotes pressing the "d" key, and "2" denotes pressing the "l" key. The model is made to predict labels 0, 1, or 2. To guarantee reliable classification performance, the model's accuracy is validated during the training phase. The eGUI presented in-front of particular subjects can be seen in figure 2.

Once a good model has been created, key press simulation comes next. The trained model is integrated with a tkinter-based Graphical User Interface (GUI) to create this simulation. Based on the recorded EEG signals, the model predicts and simulates key presses and the GUI imitates the FreeForm-interaction eGUI screen. Through the completion of this extensive procedure, which includes data collection and preprocessing, model training, validation, and simulation, the project hopes to aid in the creation of a dependable system for brain-computer interfaces. The ultimate objective is to offer a neurodegenerative disability support system that will improve the user's capacity to engage with digital platforms by means of an EEG-controlled virtual keyboard.



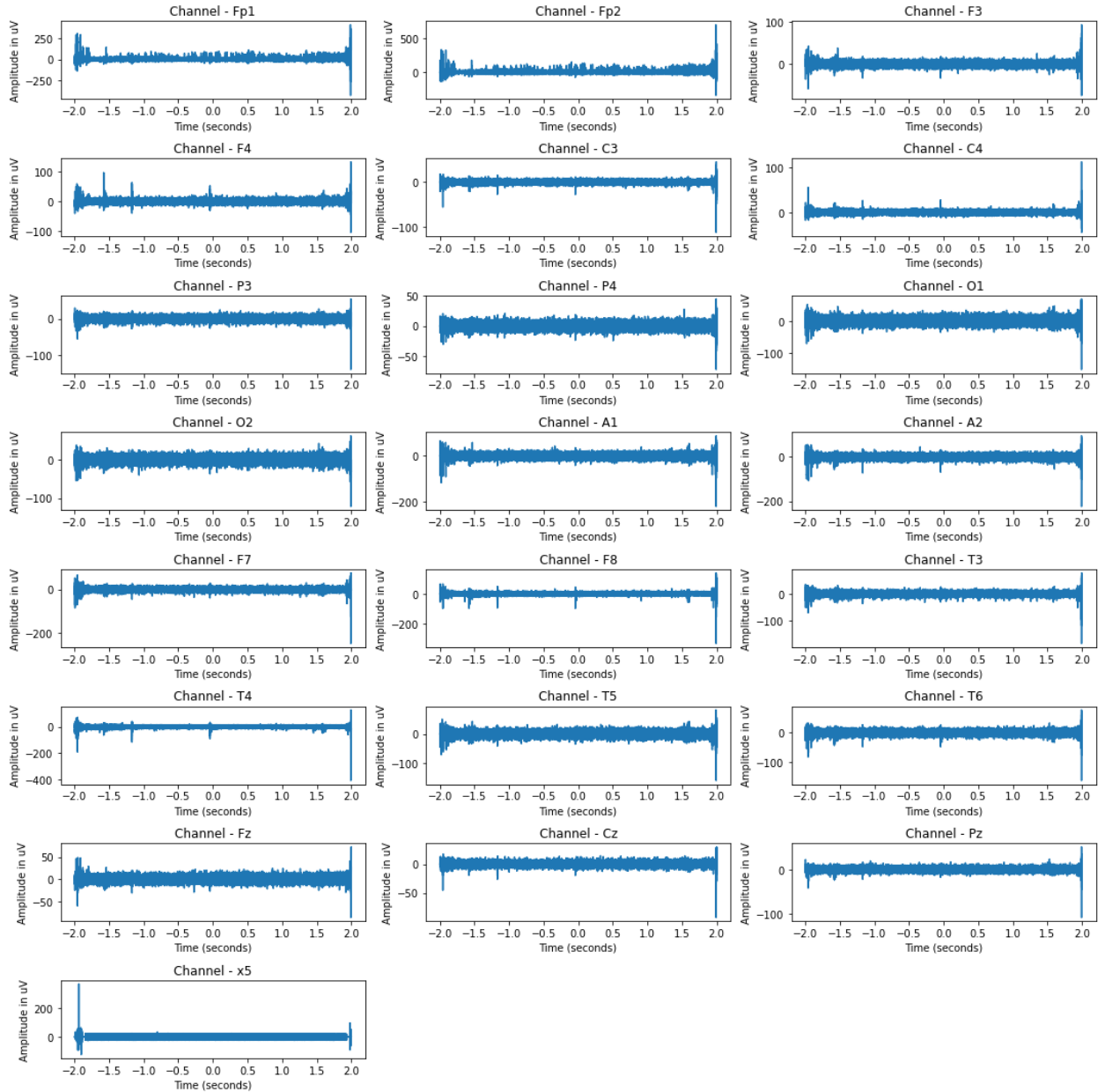


**Fig 3.** Visualization of the dataset

The figure 3. displays a 22-channel electroencephalogram (EEG) recording, with each subplot representing the brain's electrical activity as recorded by scalp electrodes. The channels are designated according to the worldwide 10-20 system, which includes positions like Fp1, Fp2, F3, F4, C3, C4, P3, P4, O1, O2, A1, A2, F7, F8, T3, T4, T5, T6, Fz, Cz, Pz, and an extra channel named X5. The channels correlate to different regions of the brain. The electrical potential of the brain is represented by each subplot, which shows the amplitude in microvolts (V) on the vertical axis and the time in seconds on the horizontal axis over a 2-second interval.

The EEG signals have been pre-filtered to eliminate high-frequency noise and artifacts, as evidenced by their apparent smoothness with some noise. Each channel's signals are comparatively steady, devoid of noticeable spikes or anomalies, indicating that the EEG data has been preprocessed—perhaps by bandpass filtering—to concentrate on the pertinent frequency bands that are frequently linked to brain activity. By minimizing the impact of outside electrical noise and physiological distortions like eye blinks or muscle movements, this preprocessing phase proved essential

for improving the quality of EEG signals and making sure the data is more indicative of the underlying cerebral activity. The redundant channels A1, A2, and X5 were removed with reference to the 10-20 system, and the preprocessing enabled the authors to create models with greater consistency. The reason for omitting the 3 channels is described in table 2.

**Table 2.** Omitted channels in the research study

Channel	Reason for Omission
<b>A1</b>	The A1 channel, located at the left earlobe or mastoid in the 10-20 system, was omitted due to no good significance earlobes or mastoids, affecting its reliability in capturing brain activity.
<b>A2</b>	The A2 channel, corresponding to the right earlobe or mastoid in the 10-20 system, was excluded because it too doesn't have a great significance as placed on earlobes or mastoids, reducing its usefulness for ML model training.
<b>X5</b>	The X5 channel was not a standard EEG electrode in the 10-20 system and was primarily used for detecting movement or capturing EEG signals during specific conditions like sleep studies. It was not relevant to the primary focus of the research and thus omitted.

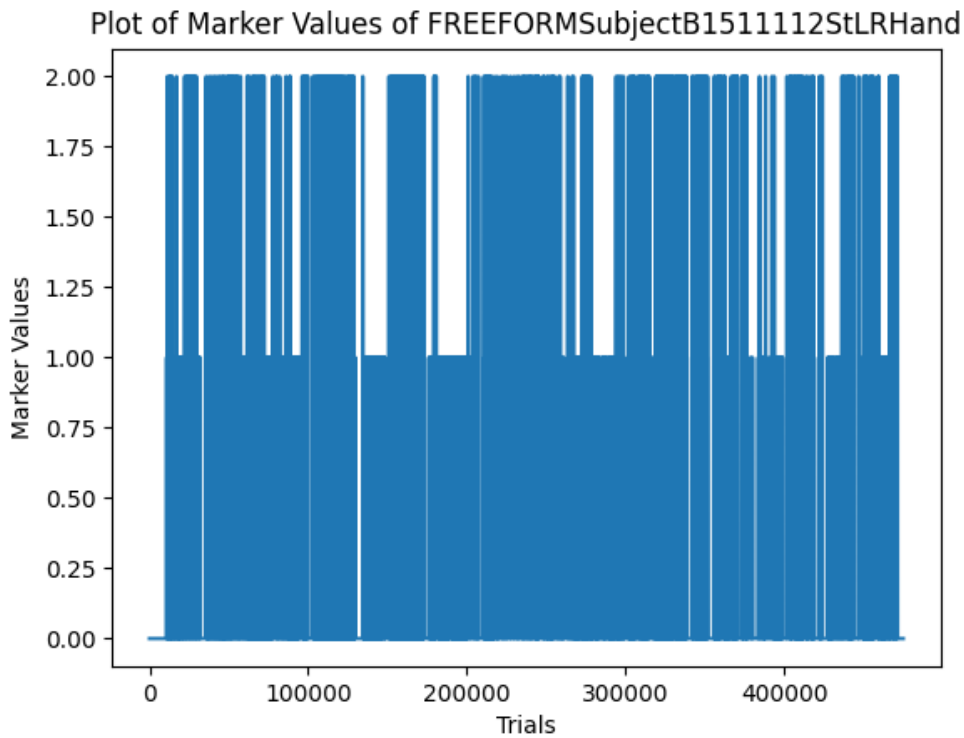


**Fig 4.** Event plot

Figure 4. shown events plot for freeform Subject B1511112StLRHand gives us important information about the activities and events that took place during the recording session. "0," which denotes the resting state, is obtained when the "d" and "l" presses are made simultaneously. This allows us to observe that the volunteer participating in the recording session is initially in a resting state and other corresponding activities are initialized as the session progresses.

### ERP analysis

We plotted the event-related potentials of 19 electrode data and analyzed the neural activity patterns, related to key press. ERP's provide us average electrical activity of the brain in response to specific stimuli or event. The utilization of ERP plots aids in the identification of distinctive features and characteristics in the EEG data that correspond to motor planning and execution. These plots can reveal subtle changes in brain activity in the time domain, particularly in the moments immediately preceding the key presses. Analyzing ERPs helps in determining the temporal dynamics of the brain's response to motor intentions, which is crucial for feature extraction and model training.

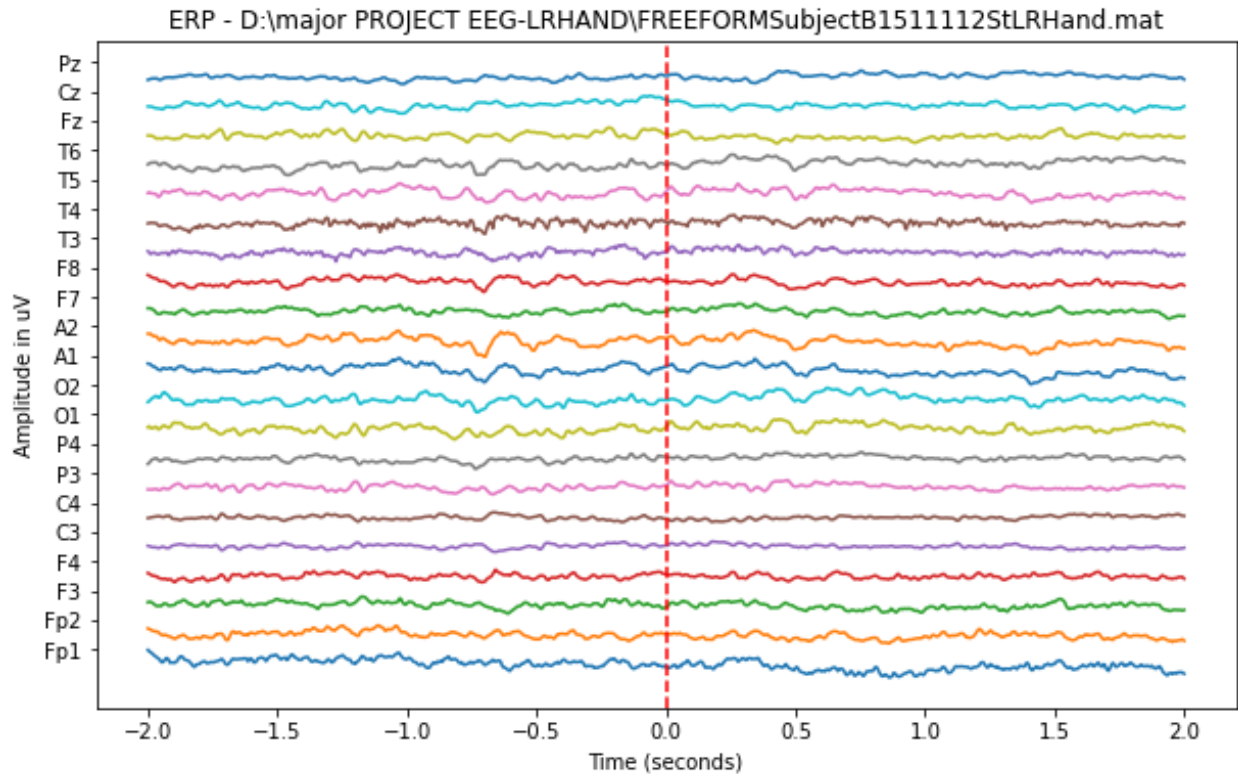


**Fig 5. ERP plot visualization**

The ERP plot is shown in figure.5. shows the 21-channel EEG data plot concerning movement onset, which provide us with the behavior of the events in the recording session. The sampling frequency of 200 hz is utilized to grab the samples and make analysis of EEG data. The event-related potential (ERP) waveforms of a (FREEFORMSubjectB1511112StL) during a freeform task are displayed in the figure above. Plotting of the ERP waveforms for 19 electrodes on the subject's scalp is done with the ERP amplitude on the y-axis and the time axis on the x-axis.

The ERP provides information about the subject's brain activity during the freeform task. The peaks and valleys in the waveforms indicate various electrical activity patterns, and the various colors correspond to various scalp electrodes. For instance, the Pz electrode, which is located at the top of the head, exhibits a positive peak at approximately 300 milliseconds, which is commonly connected to the ERP's P300 component. It is believed that the P300 component reflects the subject's focus on the freeform task.

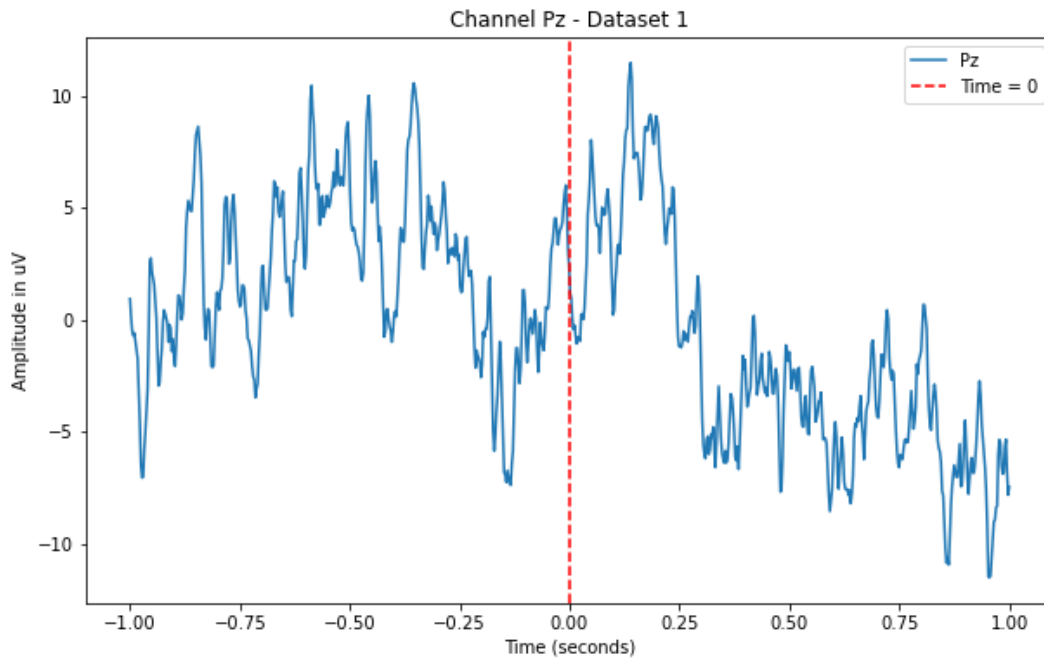


**Fig 6. ERP plot of channel Pz of dataset-1**

The figure 6. shows an event-related potential (ERP) waveform for a single channel (Pz) of a dataset. The ERP is a measure of the electrical activity of the brain in response to a specific event or stimulus. It is calculated by averaging the EEG data from multiple trials, which cancels out random noise and reveals the underlying brain response. The ERP waveform is typically characterized by a series of peaks and troughs, each of which is associated with a different stage of cognitive processing. For example, the P1 wave is thought to reflect the initial sensory processing of a stimulus, while the N1 wave is thought to reflect the attention to that stimulus. Later waves, such as the P300 and N400, are thought to reflect higher-level cognitive processes, such as decision-making and memory retrieval. The specific ERP waveform that is observed can vary as it is dependent on the type of stimulus or event that is presented. For example, the ERP waveform for a visual stimulus will be different from the ERP waveform for an auditory stimulus. The ERP waveform can also be affected by the individual's cognitive state, such as their attention level or fatigue.

The y-axis of the graph is in microvolts (uV), and the x-axis is in seconds. The graph shows a negative voltage deflection, or ERP (event-related potential), that peaks around 200 milliseconds after the stimulus. This ERP is called the P2 component. The P2 component is thought to reflect the brain's automatic processing of sensory stimuli. It is larger for attended stimuli than for unattended stimuli, and it is also sensitive to the complexity of the stimuli. The specific meaning of the P2 component is associated with the Keypress events in the context of this project. For example, as the stimuli were words, the P2 component is larger for words that are attended to or that are unexpected. Overall, the image suggests that the participants in the experiment were paying attention to the stimuli and that their brains were processing them automatically. The ERP analysis visualizations for all channels are shown in figure 7.

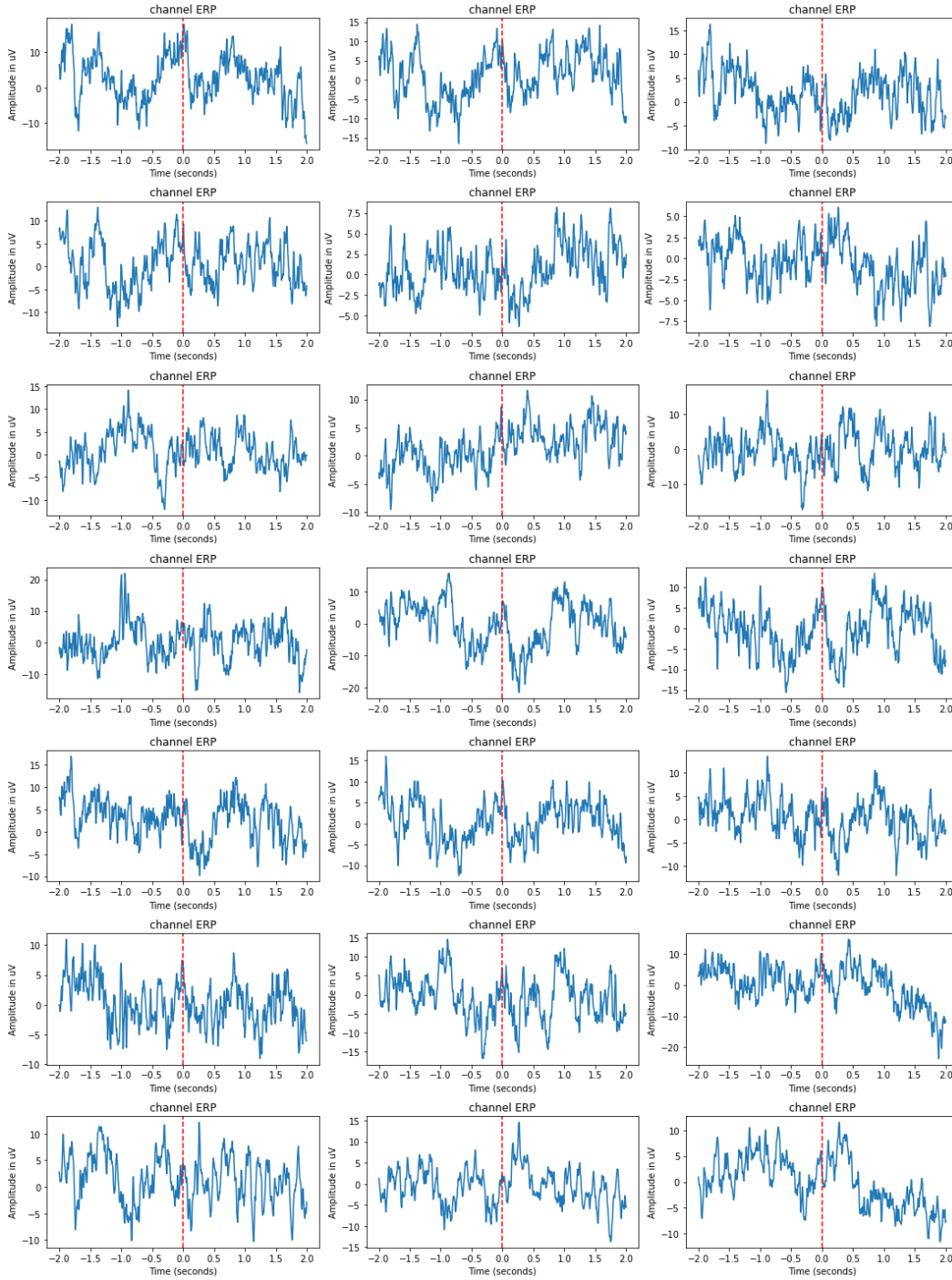


**Fig 7.** ERP plot visualization for all the channels

## Basic Architecture

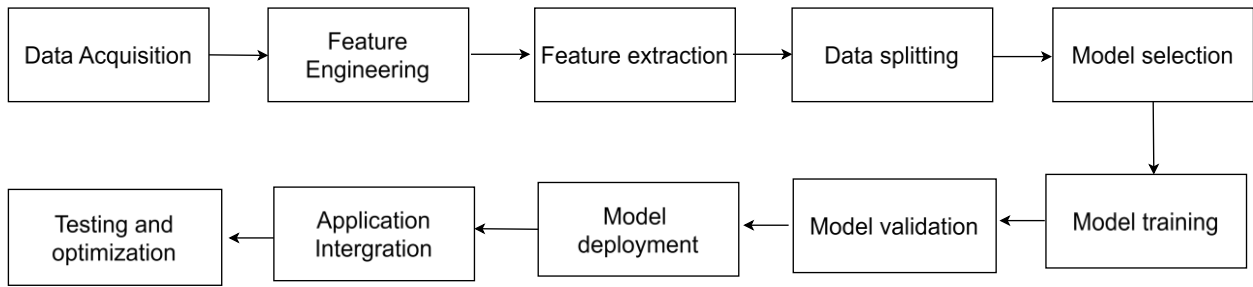


**Fig 8. Proposed architecture**

1. **Data Acquisition:**

As, shown in block diagram in figure 8. first stage is to obtain the EEG dataset from the FreeForm paradigm in Nature, which captures neural activity related to voluntary motor movements before key presses. Then, we extract relevant information, including EEG signals, key press events, and associated labels (0 for blank, 1 for 'd' key press, and 2 for 'l' key press).

2. **Data Preprocessing:**

We Segment the EEG data into trials aligned with key press events. We identify and visualize events using event plots with markers, ensuring accurate alignment. Then, we utilize ERP plots to observe and analyze neural activity changes preceding key presses.

3. **Feature Engineering:**

We extract relevant features from the preprocessed EEG data. We consider time-domain and frequency-domain features that capture meaningful patterns in the neural signals.

The acquired EEG signal was not subjected to any special filtering as it was preprocessed, so the above block diagram omits the preprocessing step. All EEG data captured at 200 Hz sampling rate in the Neurofax program had a band-pass filter of 0.53–70 Hz. The Neurofax software's largest band-pass filter selection, which ranges from 0.53 to 100 Hz, was used to process the EEG recordings that were obtained at a sampling rate of 1000 Hz. Since these are hardware filters, they are included in all records that have been made public. The EEG-1200 hardware also has a 50 Hz notch filter to lessen electrical grid interference [6]. We finally segment the dataset into 19-electrode data, removing two channels that do not have a primary role in the brain activity-based control. The ERP window-based data segmentation was done with those below Event 0 belonging to one and above Event 0 belonging to another window so that total electrode-based data division resulted in a total of 19\*3800 data arrays. A list of file paths (`mat_file_paths`), each of which represents a MATLAB file containing EEG data, is iterated over by the proposed script. It loads the data from each file and uses the `process_data()` function to process it. Further processing is carried out if the required information and labels are present.

4. **Feature Extraction and Data Saving:** We extracted EEG features for each class onset found in the marker data during the processing loop. To achieve this, we defined a window around each onset and pulled out EEG data from a predetermined window that includes the onset and its aftermath. Following their extraction, these features were arranged into rows and added to a list (`rows_list`) together with their respective class labels. And finally, the dataset was saved.

5. Data Splitting:

We Split the dataset into training and validation sets to facilitate model training and evaluation.

6. Model Selection:

We choose an appropriate machine learning model for the classification task. In this case, the deep learning model is selected due to its ability to capture temporal dependencies in sequential data.

7. Model Training:

Training the model using the training dataset is carried out. We optimize hyperparameters to improve model performance. We utilize techniques such as dropout to prevent overfitting.

8. Model Validation:

We validate the trained model using the validation dataset. We then, evaluate metrics such as accuracy, precision, recall, and F1-score to assess classification performance.

9. Simulation Integration:

We develop a tkinter-based GUI that replicates the FreeForm-interaction eGUI screen and then, integrate the trained model with the GUI for real-time prediction of key presses based on incoming EEG signals.

10. Simulation Testing:

We Simulate key presses using the integrated model and GUI. Then we verify the accuracy of simulated key presses against the actual recorded key presses.

11. Optimization and Iteration:

We then, fine-tune the model and GUI based on simulation results and user feedback. We iterate through the training and validation steps to enhance model accuracy and generalization. The model practical usage is illustrated in figure 9.

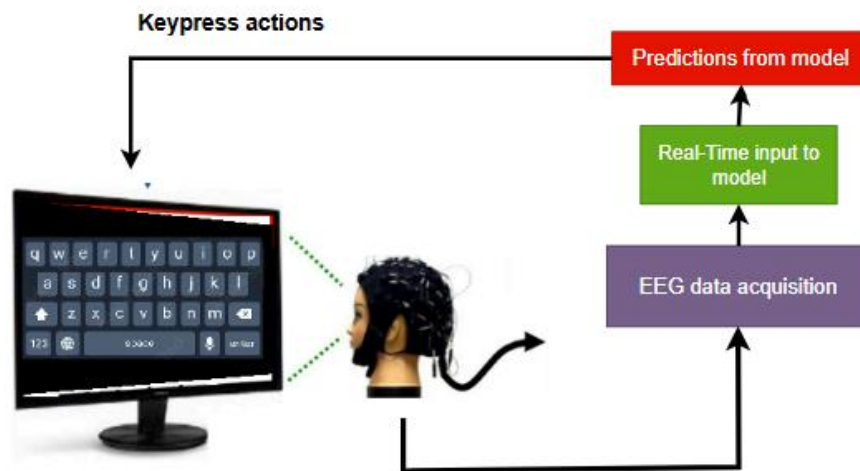


**Fig 9.** Model deployment with practical usage

## Algorithms

*Algorithm for BCI-Based Virtual Keyboard:*

Step 1: Data Preprocessing

Input:

EEG dataset from the FreeForm paradigm.

Key press events (timestamps and labels).

Process:

Segment EEG data into trials based on key press events.

Align events and visualize using event plots with markers.

Apply ERP analysis and potential signal filtering for data enhancement.

Output:

Preprocessed EEG data with labeled events.

Step 2: Feature Engineering

Input:

Preprocessed EEG data.

Process:

Extract relevant features from EEG signals.

Apply onset window-based segmentation using a sampling rate

Output:

Feature-rich dataset for model training.

Step 3: Data Splitting

Input:

Feature-rich dataset.

Process:

Split the dataset into training and validation sets.

Output:

Training and validation datasets.

Step 4: Model Training

Input:

Training dataset.

Process:

Choose deep learning architecture for temporal sequence learning.

Train the model using backpropagation and optimization techniques.

Output:

Trained Deep learning model.

Step 5: Model Validation

Input:

Validation dataset.

Process:

Validate the model using metrics like accuracy, precision, recall, and F1-score.

Output:

Validation metrics and insights.

Step 6: Simulation Integration

Input:

Trained DEEP LEARNING model.

Tkinter-based GUI.

Process:

Integrate the model with the GUI for real-time prediction.

Capture incoming EEG signals in real-time.



Output:  
Real-time predictions of key presses.

#### Step 7: Simulation Testing

Input:  
Real-time predictions.  
Actual key press events.  
Process:  
Simulate key presses using the GUI.  
Compare simulated and actual key presses for accuracy.  
Output:  
Simulation results and accuracy metrics.

### Proposed Model

#### Support Vector Machine (SVM model)

For problems involving regression and classification, supervised machine learning algorithms such as Support Vector Machines (SVM) are employed. An SVM divides the data points into classes by building a hyperplane, or collection of hyperplanes, in a high-dimensional space. The SVM's goal is to identify the hyperplane that maximizes the margin—that is, the distance between the hyperplane and the support vectors, or closest data points—for each class.

When there are more characteristics than samples and high-dimensional spaces, SVMs perform especially well. They can employ a variety of kernel functions, including linear, polynomial, radial basis function (RBF), and sigmoid kernels, to handle both linear and non-linear classification tasks. The model architecture can be seen in figure 10.

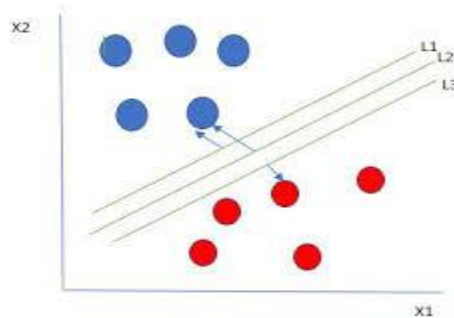


**Fig 10.** SVC (Support vector classifier) architecture

#### Logistic Regression

When attempting to estimate the likelihood of a binary outcome, such as true or false, based on one or more input features, a statistical technique called logistic regression is employed. Logistic regression which graph has been shown in figure 11. models the likelihood that a given input belongs to a specific class by using the logistic function, also called the sigmoid function, as opposed to linear regression, which predicts a continuous result.

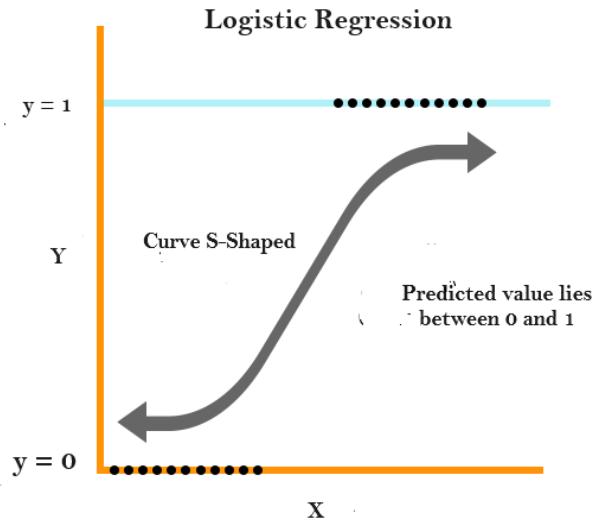


**Fig 11.** Logistic Regression graph

Multinomial logistic regression estimates three sets of coefficients, one for each class, in a three-class problem. The model forecasts the likelihood that an instance will belong to each of the three classes rather than a binary result. The class with the highest probability is selected as the anticipated label as the sum of these probabilities is always equal to one.

**MLP (Multi-Layer Perceptron)**

Because of its capacity to handle complicated patterns in data, the Multilayer Perceptron (MLP) algorithm is a crucial kind of Artificial Neural Network (ANN) that is widely employed in machine learning. Activation functions such as sigmoid, tanh, or ReLU are used by multilayer pyramids (MLPs) to incorporate non-linearity and capture complex relationships in data. MLPs consist of layers of interconnected nodes, including an input layer, one or more hidden layers, and an output layer. MLPs are useful for a variety of tasks, including regression issues image identification and sentiment analysis. They are trained using backpropagation and iteratively modify weights to decrease prediction errors.

MLPs shown in figure 12. are flexible and can learn non-linear mappings, but they can be computationally demanding, especially when dealing with larger datasets and more intricate designs. To avoid overfitting, parameters must be carefully adjusted. Nevertheless, MLPs are a mainstay of neural network applications due to their versatility and efficacy, which are always changing in tandem with developments in deep learning methodologies.

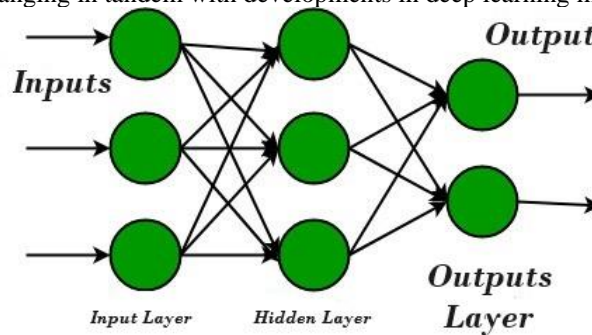


**Fig 12.** MLP architecture

**Bi-Directional LSTM-GRU (Bi-Directional Long Short Term Memory-Gated Recurrent Unit) hybrid model**

The model we proposed is a deep learning model for classification, leveraging both LSTM and GRU layers within a Bidirectional architecture. It is designed to handle sequential data, making it suitable for time series or any data where context from previous steps is valuable. The model is built using the TensorFlow Keras API and trained using a cross-validation approach to ensure robust performance. The architecture begins with a Bidirectional LSTM layer, followed by a dropout layer for regularization, and then a Bidirectional GRU layer, another dropout layer, and a dense output layer with softmax activation for classification. The training process includes standardization of features, early stopping based on validation loss, and plotting accuracy and loss for each fold to monitor training progress. The model architecture can be seen in figure 13.

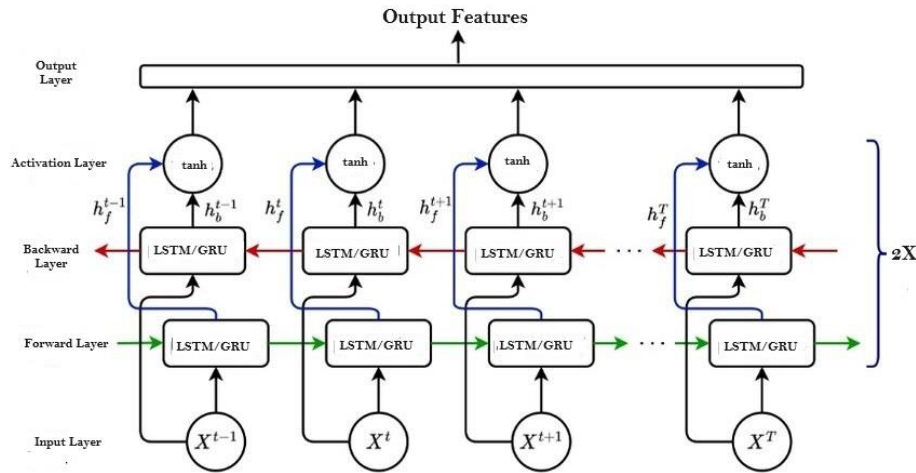


**Fig 13.** Bi-directional LSTM GRU hybrid model architecture

### Batch Size

Batch size is the number of training examples utilized in one iteration of the model's training process. Instead of updating the model weights after each individual example (which can be noisy) or after the entire dataset (which can be slow), the weights are updated after processing a subset (batch) of the dataset.

### Loss Function

A loss function, also known as a cost function or objective function, is a method of evaluating how well the model's predictions match the true data labels. It measures the difference between the predicted output and the actual output.

### Adam Optimizer

Adam (short for Adaptive Moment Estimation) is an optimization algorithm used to update the network weights iteratively based on training data. It combines the advantages of two other extensions of stochastic gradient descent: AdaGrad and RMSProp.

### L2 Regularization

L2 regularization, also known as weight decay, is a technique to prevent overfitting by adding a penalty to the loss function proportional to the square of the magnitude of the weights. This discourages the model from fitting the noise in the training data by keeping the weights small.

## Dropout

Dropout is a regularization technique where, during each training iteration, a fraction of the input units to a layer is randomly set to zero. This prevents units from co-adapting too much, encouraging the network to learn more robust features.

## Catboost

CatBoost (Categorical Boosting), is one of the newer machine learning algorithm that excels at managing categorical information. It performs well in both classification and regression problems and is a member of the gradient-boosting algorithm family. With its high efficiency design, CatBoost can achieve great accuracy even with default parameters and quick training times with help of various learners shown in figure 14. Given that it accepts categorical variables directly and does not require one-hot encoding, it also reduces the requirement for costly data pretreatment.

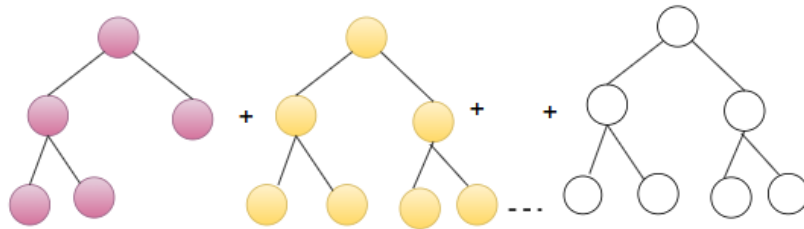


Fig 14. Catboost algorithm architecture

## K- Nearest Neighbours (KNN)

A straightforward, instance-based, non-parametric learning technique, K-Nearest Neighbors (KNN) is mostly utilized for regression and classification applications. Data points are categorized using the KNN method according to the feature space's K nearest neighbors' majority class. Although it is simple to use and comprehend, the computation of the distances to each point in the dataset can be costly when dealing with huge datasets. KNN shown in figure 15. performs best in scenarios where the data is noise-free, small, and has well-defined classes.



Fig 15. KNN algorithm architecture

## Gaussian Naïve Bayes

Based on Bayes' Theorem and the assumption that the characteristics have a Gaussian (normal) distribution, Gaussian Naive Bayes is a probabilistic classification algorithm. The Naive Bayes classifier, of which this variant is a variation, makes the assumption that all features, given the class label, are independent of one another. Despite this oversimplifying presumption, Gaussian Naive Bayes has a lot of potential for success, particularly with high-dimensional datasets. Its simplicity and effectiveness make it a popular choice for text classification, spam detection, and medical diagnosis. The architecture is shown in figure 16.

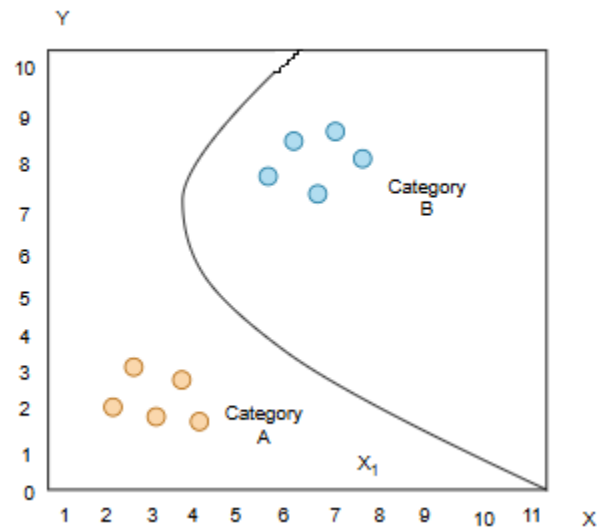


Fig 16. Gaussian Naïve Bayes architecture

## Models Performance Evaluation Metrics

### Hyperparameter Tuning

The process of determining a machine learning algorithm's ideal hyperparameters is known as hyperparameter tuning. Hyperparameters are those that are predetermined and cannot be discovered by data-driven analysis during the training phase. The regularization parameter in linear models, the learning rate in neural networks, and the depth of decision trees are a few examples of hyperparameters.

The process of hyperparameter tuning entails utilizing methods like grid search, random search, or more sophisticated optimization algorithms like Bayesian optimization to search over a predetermined range of hyperparameters. The objective is to determine which set of hyperparameters gives the model the highest performance either through cross-validation or on a validation set.

### 10-Fold stratified cross validation

A method for evaluating how effectively a prediction model generalizes to a separate dataset is cross-validation. The original dataset is split into  $k$  equal-sized subsets, or folds, for  $k$ -fold cross-validation. On  $k-1$  folds, the model is trained, and on the remaining fold, it is validated. This procedure is carried out  $k$  times, with a distinct fold serving as the validation set each time. To get an approximation of the total performance, the performance measures are then averaged over the  $k$  iterations.

**Mean (Average):** The mean, also called the average, is a central tendency measure that is calculated by dividing the total number in a set by the total number in the set. It is frequently used to provide a single representative value by summarizing a dataset. The data's outliers can affect the mean.

**Standard Deviation (SD):** A measure of a group of values' dispersion or spread around the mean is the standard deviation. It shows the degree to which a dataset's values diverge from the mean. A high standard deviation suggests that the values are dispersed over a larger range, whereas a low standard deviation suggests that the values tend to be near the mean.

**Confusion Matrix:** A table used to assess a classification model's performance is called a confusion matrix. It displays an overview of the model's predictions in comparison to the actual factual values. The actual class is represented by each row in the matrix, whereas the anticipated class is represented by each column. True Positive (TP), False Positive (FP), True Negative (TN), and False Negative (FN) are the four quadrants of the confusion matrix.

**F1-Score:** statistic provides a single assessment of a model's effectiveness in binary classification tasks by combining precision and recall. The harmonic mean of recall and precision is used to calculate it. When there is an imbalance between the classes in the dataset, the F1-score is helpful since it balances false positives and false negatives as given by equation 1.

$$F1\ Score = 2 \times \frac{Precision * Recall}{Precision + Recall} \dots \dots \dots \text{Equation 1.}$$

**Recall (Sensitivity):** A model's capacity to accurately identify every pertinent instance of a class is gauged by the recall, which is also referred to as sensitivity or true positive rate. The ratio of true positives to the total of false negatives and true positives is used to compute it. A high recall suggests that the model reduces false negatives well as given by equation 2.

$$Recall = \frac{TP}{(FN+TP)} \dots \dots \dots \text{Equation 2.}$$

**Precision:** Precision is the capacity of a model to accurately identify, out of all the examples it has identified as belonging to a class, only the relevant instances of that class. The ratio of true positives to the total of true positives and false positives is used to compute it. A high precision means that the model reduces false positives as well as possible and is given by equation 3.

$$Precision = \frac{TP}{(FP+TP)} \dots \dots \dots \text{Equation 3.}$$

**Accuracy**

Accuracy is the proportion of cases that were accurately predicted in all instances. It is given by equation 4.

$$Accuracy = \frac{TP+TN}{(FP+FN+TP+TN)} \dots \dots \dots \text{Equation 4.}$$

**Classification Report:**

A report on classification gives a summary of a model's performance across multiple classifications. Typically, metrics like support for each class, accuracy, recall, and F1-score are presented. The report provides insights into the model's performance for each class, which can help identify areas where the model may need to be developed.

**Hardware required**

As, this project is completely based on EEG data classification, in which the dataset is obtained from a nature journal publication and project is finally developed with an ML model so, no hardware component is used here.

## RESULTS AND DISCUSSIONS

After successive data cleaning and feature engineering for 19-electrode data from EEG signals, we could classify them into rows and columns and subject C-I, and Subject C-II datasets were utilized for training, and similarly, for validation subject B dataset was utilized. The acquired EEG signal was not subjected to any special filtering. All EEG data captured at a 200 Hz sampling rate in the Neurofax program had a band-pass filter of 0.53–70 Hz. Since these are hardware filters, they were included in all records that have been made public. The EEG-1200 hardware also has a 50 Hz notch filter to lessen electrical grid interference [6]. The preprocessing and feature extraction was supported due to its pre-filtering and the Model was tested with different hyperparameters and a high linearity was seen on the SVM model for choosing Kernel as 'linear'. The model result of nearly 89% accuracy on mean validation shows that how well the model performs on classifying the '0', '1' and '2' class i.e. different keypress events ('rest', 'd' and 'l' finally).

### Gaussian NB:

**Table 3.** Gaussian Naiver Bayes stratified cross-validation results

Fold	Testing Accuracy
Fold 1	0.7878
Fold 2	0.7950
Fold 3	0.8237
Fold 4	0.7878
Fold 5	0.7986
Fold 6	0.7590
Fold 7	0.8159
Fold 8	0.7906
Fold 9	0.7690
Fold 10	0.7942
Mean Testing Accuracy	0.7921
Standard Deviation	0.0181

The testing accuracy for Gaussian Naïve at 10 distinct folds during a cross-validation procedure is summarized in the table 3. There is a small variation in the testing accuracy for each fold; the numbers range from 0.7726 to 0.8123. The model's average performance on the test data is indicated by the mean testing accuracy of 0.7921 across all folds. With very slight variations around the mean, the accuracies are comparatively stable, as indicated by the standard deviation of 0.0181. This means that overall, the model's performance is steady and dependable, and it performs pretty uniformly across various data subsets, the hyperparameters used can be seen in table 4.

**Table 4.** Hyperparameters for Gaussian Nabiers model

Hyperparameter	Value
Number of Splits (n_splits)	10
Shuffle	True
Random State	42
Standard Scaler	StandardScaler()
Model	GaussianNB()

### Catboost results:

The boost model obtained an accuracy of 88% on testing and 100% on training set and further evaluation with stratified 10-fold cross validation following results as shown in the table were obtained as seen in table 5.

**Table 5.** 10-fold accuracies for Catboost model

Fold	Testing Accuracy
Fold 1	0.8705
Fold 2	0.8741
Fold 3	0.8885
Fold 4	0.8597
Fold 5	0.8777
Fold 6	0.8345
Fold 7	0.9061
Fold 8	0.8773
Fold 9	0.8412
Fold 10	0.9097
Mean	0.8739
Standard Deviation	0.0232

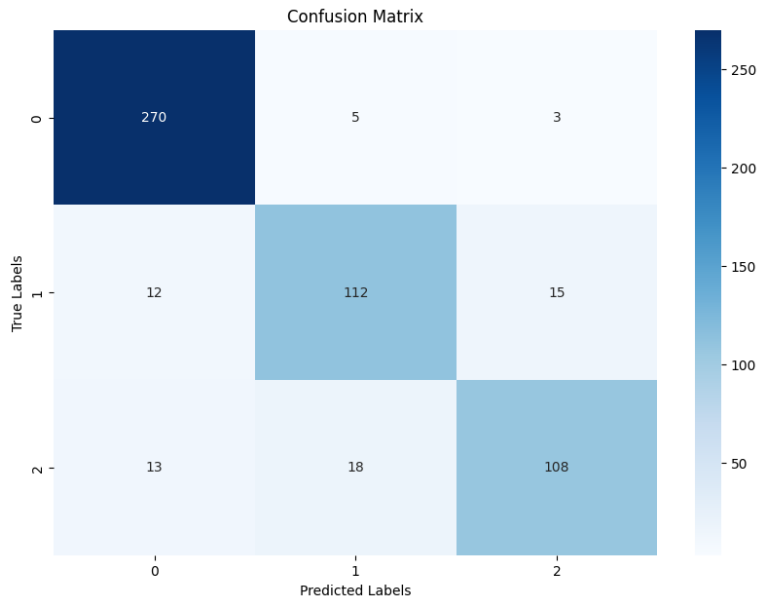


**Fig 17.** Confusion matrix plot for catboost model performance

The confusion matrix plot as shown in the figure 17. shows very good results with 262 instances out of 278 total predicted correctly for class '0' which is the rest state, similarly, out of total of 139 instances 120 were predicted correctly as class 1 is keypress 'd' action and finally, out of total 139 instances for class '2' the 120 instances were predicted correctly as class 3 which is keypress 'l' action. This shows the great performance and reliability of utilizing catboost on classifying the EEG-based events and hyperparameters used is shown in table 6.

**Table 6.** Hyperparameters for boost model

Hyperparameter	Value
iterations	1000
depth	6
learning_rate	0.1
loss_function	MultiClass
eval_metric	Accuracy
verbose	False



random_seed	42
-------------	----

## KNN Algorithm

The KNN model obtained an accuracy of 72% and the detailed testing accuracies of each folds can be seen in table 7.

**Table 7.** Cross validation results of KNN algorithm

<b>Fold</b>	<b>Testing Accuracy</b>
Fold 1	0.7158
Fold 2	0.7302
Fold 3	0.7482
Fold 4	0.7374
Fold 5	0.7014
Fold 6	0.6906
Fold 7	0.7292
Fold 8	0.7437
Fold 9	0.7040
Fold 10	0.7581
<b>Mean Testing Accuracy</b>	<b>0.7259</b>
<b>Standard Deviation of Accuracy</b>	<b>0.0211</b>

: The KNN algorithm performance as shown in the table over ten folds demonstrates a continuously medium degree of accuracy. The testing accuracy varies from 70% to 74% for each fold, indicating the resilience and dependability of the model in classification tasks. With a comparatively low standard deviation of 0.0211 and a mean testing accuracy of 972.59% across all folds, the model appears to have continuous good performance across all data subsets. The model is a dependable option for the given classification problem because of its little variability in accuracy over folds, which shows that it maintains excellent performance even when exposed to varied training and testing sets. The hyperparameters utilized can be seen in table 8.

**Table 8.** Hyperparameters for KNN algorithm

<b>Hyperparameter</b>	<b>Value</b>
Shuffle	True
Standard Scaler	StandardScaler()
Model	KNeighborsClassifier
Number of Neighbors (n_neighbors)	5
Weights	'distance'
Algorithm	'auto'
Power Parameter (p)	2

## Logistic Regression

The model logistic regression obtained an accuracy of 100% on training and with cross-validations on the test set an accuracy of 90% is obtained. Each fold accuracies can be seen in table 9.

**Table 9.** Model logistic regression accuracy results included:

<b>Fold</b>	<b>Testing Accuracy</b>
1	0.8957
2	0.9209
3	0.9245

4	0.8813
5	0.9317
6	0.9029
7	0.9386
8	0.8881
9	0.8736
10	0.9242
<b>Mean</b>	<b>0.9081</b>
<b>Standard Deviation</b>	<b>0.0216</b>

The Logistic Regression model's performance as shown in table over tenfold demonstrates a continuously high degree of accuracy. The testing accuracy varies from 87.36% to 93.86% for each fold, indicating the resilience and dependability of the model in classification tasks. With a comparatively low standard deviation of 0.0216 and a mean testing accuracy of 90.81% across all folds, the model appears to have continuous good performance across all data subsets. The model is a dependable option for the given classification problem because of its little variability in accuracy over folds, which shows that it maintains excellent performance even when exposed to varied training and testing sets. The different hyperparameters used can be seen in table 10.

**Table 10.** Hyperparameters for Logistic Regression model

<b>Hyperparameter</b>	<b>Value</b>
Penalty	'l2'
Inverse Regularization (C)	0.1
Solver	'saga'
Max Iterations (max_iter)	200
Multi-Class Handling	'auto'
Random State	42

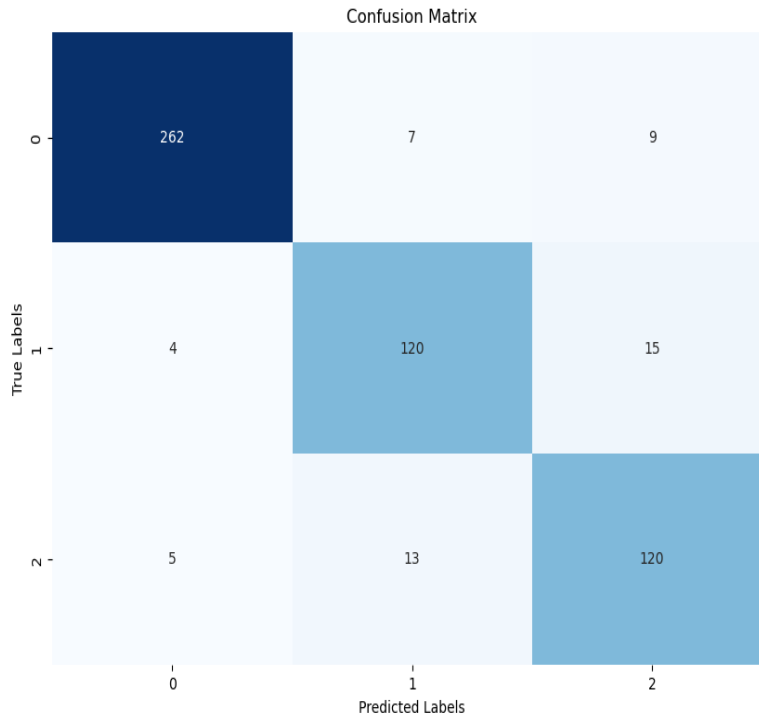


**Fig 18.** Confusion matrix plot for Logistic Regression

The confusion matrix plot as seen in figure 18 shows very good results with 262 instances out of 278 total predicted correctly for class '0' which is the rest state, similarly, out of a total of 139 instances 120 were predicted correctly as class 1 is keypress 'd' action and finally, out of total 139 instances for class '2' the 120 instances were predicted correctly as class 3 which is keypress 'l' action. This shows the great performance and reliability of utilizing the logistic regression model on classifying the EEG-based events even though the algorithm is quite old, but still has great support for such a complex evaluation.

### **SVM model results**

The SVM model achieved 98.02% on training and similarly, 90.29% on testing. The confusion matrix plot is shown in figure 19.

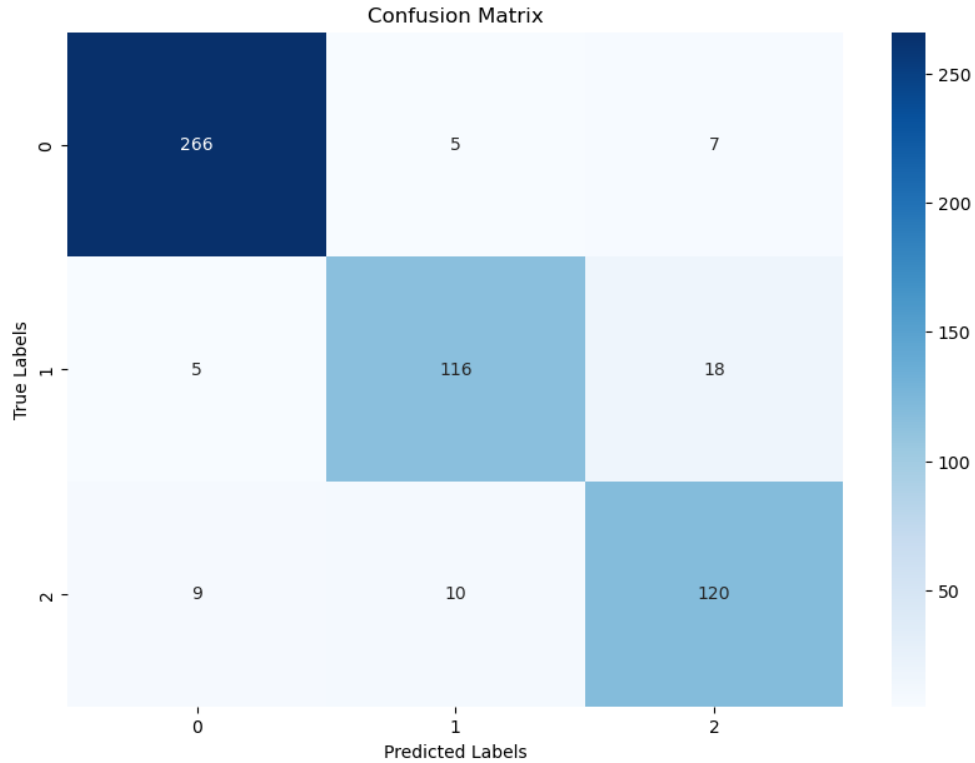


**Fig 19.** Confusion Matrix plot

The confusion matrix plot for the SVC model is shown in figure 19. The confusion matrix plot as shown in the figure shows very good results with 266 instances out of 278 total predicted correctly for class '0' that is the rest state, similarly, out of a total of 139 instances 116 were predicted correctly as class 1 is keypress 'd' action and finally, out of total 139 instances for class '2' the 120 instances were predicted correctly as class 3 which is keypress 'l' action. This indicates very high performance for the SVC classifier. The 10 fold cross validation accuracies can be seen in table 11.

**Table 11.** 10-fold stratified validation results

Fold	Testing Accuracy
1	0.8993
2	0.8957
3	0.9173
4	0.8705
5	0.9173
6	0.8957
7	0.9314
8	0.9061
9	0.8917
10	0.9170
Mean	0.9042
Standard Deviation	0.0165

This table presents the accuracy values for each fold, and the model has gained a mean accuracy of 90% with 0.0165 as the standard deviation value which is a very good performance seen. An effective method for assessing a model's performance in machine learning is the 10-fold stratified cross-validation approach. We applied the validation for

testing the accuracy of classifying by models on different folds on the dataset of EEG features of 19 different channels. This technique divides the dataset into ten folds or equal-sized subsets. Ten times, the model is trained and assessed, with the remaining nine folds serving as the training set and a separate fold serving as the test set. Ensuring that every data point is used for testing as well as training, helps to lessen evaluation bias.

On training through the SVM machine learning model, we could obtain 89% accuracy, and similarly, on 10-fold stratified cross-validations, the model showed exceptional performance with a mean accuracy of 90.21%. The optimal hyperparameter for the SVM model that was found via successive fine-tuning with cross-validation is  $C=0.001$  as shown in table 12.

**Table 12.** Best Hyperparameter for SVM model

Hyperparameter	Value
C	0.001
Kernel	Linear

The F1 score on the above report shows that on predicting class 0 i.e. rest state the model has been successful for predicting class 0 exceptionally well and similar for class 1 and class 2. A set of values' variability or dispersion is measured by the standard deviation. In this case, the degree of variation in the accuracy scores over the 10 folds is indicated by a standard deviation of 2.36%. Robust generalization benefits from a low standard deviation, which indicates that the model's performance is consistent across various data subsets. Overall, the model appears to be operating effectively and stable across various subsets of the EEG signal data, as seen by its mean accuracy of 90.13 % and low standard deviation of 1.36%. This shows that the model can generalize well to fresh, untested samples and has picked up useful patterns from the data.

### Bi-Directional LSTM-GRU model results

The Bi-Directional LSTM-GRU model was trained and on successive fine-tuning of the model, an impressive accuracy of 92% was seen, while on cross-validation 90% was the mean accuracy with 0.01 as the standard deviation for the model.

The classification report for the hybrid model combining LSTM and GRU layers demonstrates strong performance across multiple metrics. The model achieves an overall accuracy of 0.92, indicating that it correctly classifies 92% of the instances. For class 0, the model shows excellent precision, recall, and F1-score, each at 0.96, reflecting its high reliability in correctly identifying instances of this class. For class 1, the precision, recall, and F1-score are all 0.89, showing consistent and balanced performance for this class. Class 2 has slightly higher precision and an F1-score of 0.90, with a recall of 0.89, indicating that the model performs well in recognizing and correctly predicting instances of this class. The macro average of precision, recall, and F1-score are all 0.92, showing that the model maintains high performance across all classes without favoring any specific class. The weighted average, which accounts for the number of instances in each class, also stands at 0.92, confirming that the model's performance is robust and balanced across the dataset. Overall, these results suggest that the hybrid model is highly effective and reliable for the classification task at hand. The 10-fold cross validation accuracies can be seen in table 13.

**Table 13.** 10-fold cross-validation results for Bi-Directional LSTM-GRU hybrid model

Fold Number	Test Accuracy
1	0.87
2	0.88
3	0.90
4	0.88
5	0.92

6	0.88
7	0.92
8	0.88
9	0.86
10	0.90
<b>Mean Test Accuracy</b>	0.89
<b>Standard Deviation of Test Accuracies</b>	0.02

Table. Hybrid model 10-fold accuracies results

The model shows a great performance with 98% on training and 89% on the testing set. The results of the 10-fold cross-validation for the Bi-Directional LSTM-GRU hybrid model, presented in Table 4.7, demonstrate consistent and robust performance across different subsets of the data. The test accuracies for each fold range from 0.87 to 0.92, indicating that the model maintains high accuracy on various splits of the dataset. Specifically, the test accuracy is 89% for folds 1 and 2, 87% for fold 3, and peaks at 92% for folds 4 and 7. The model achieves 90% accuracy in folds 5, 6, 8, and 10, and 91% in fold 9. The mean test accuracy across all folds is 90%, demonstrating that the model performs consistently well overall. The standard deviation of the test accuracies is 0.01, which is low and indicates that the model's performance is stable and does not vary significantly across different folds. These results suggest that the Bi-Directional LSTM-GRU hybrid model is reliable and effective for the classification task, with minimal variability in performance across different data subsets.

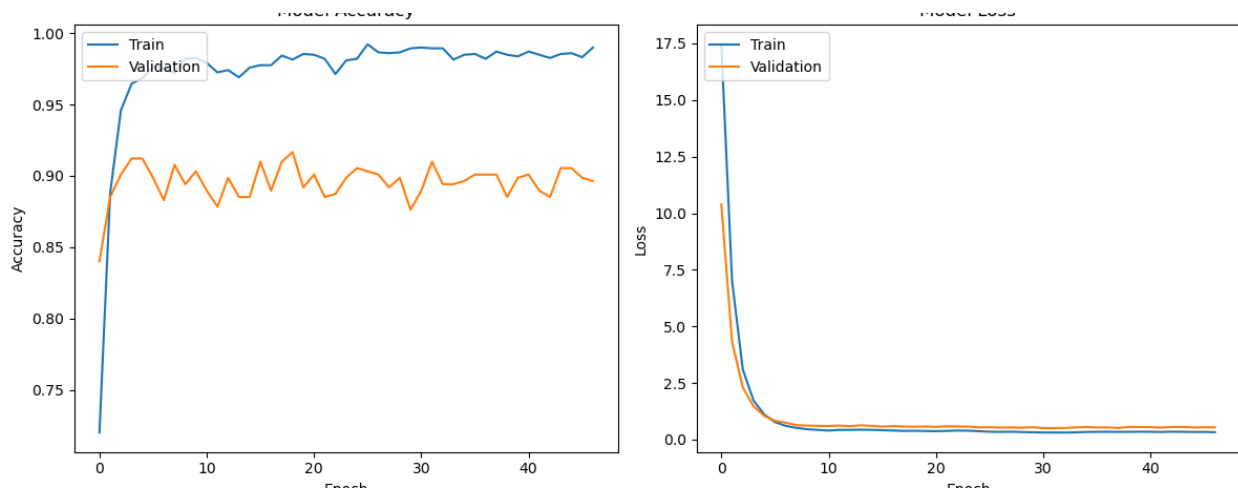
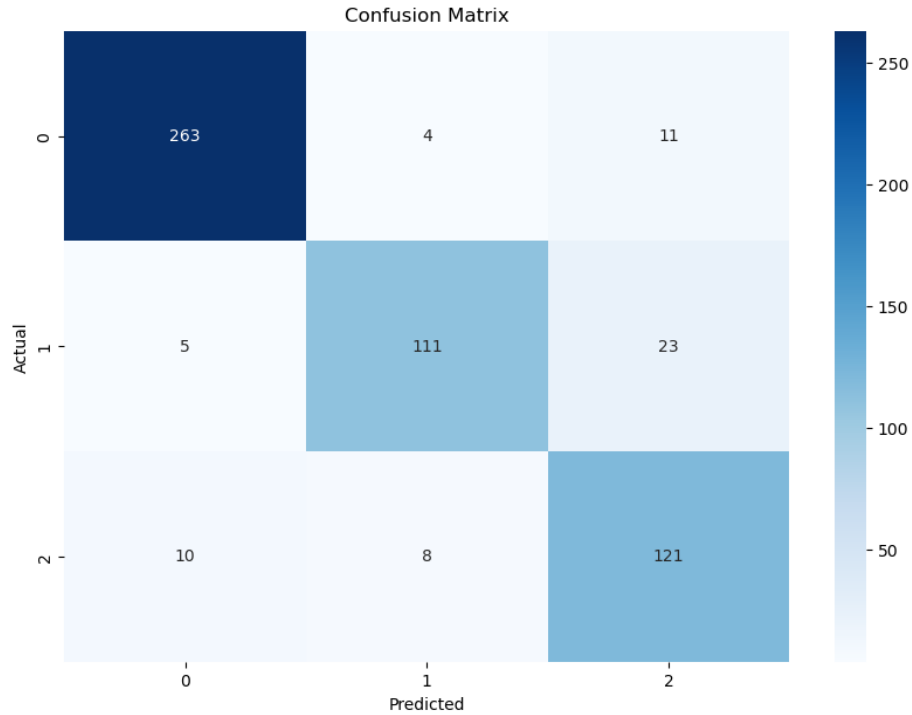


Fig. 20. Accuracy and Loss history plot for Bi-Directional LSTM-GRU hybrid model

The history plot for Bi-Directional LSTM GRU hybrid model is shown in figure 20, we can see that model performance remains good with approximate 98% training accuracy and in the graph, the x-axis represents the number of epochs, or iterations, the model has been trained. The y-axis for the accuracy plots shows what proportion of the data the model classified correctly, while the y-axis for the loss plots shows how well the model performed on a representative sample of the data it was not trained on (validation set). Looking at the accuracy plots, it can be seen that the model achieved a very high accuracy on the training data (around 96) after only a few epochs. And validation accuracy is found to be approximately 90%. Looking at the loss plots, we see a similar pattern. The training loss decreases rapidly to around 0.2. The model results suggest a very good finding overall in the model's performance.



**Fig 21.** Confusion matrix plot for hybrid model

The confusion matrix plot for the hybrid bi-directional LSTM GRU model is shown in figure 21. The confusion matrix plot as shown in figure shows the very good results: 263 instances out of 278 total were predicted correctly for class '0', which is rest state; similarly, out of total 139 instances, 111 were predicted correctly as class 1, which is keypress 'd' action; and finally, out of total 139 instances for class '2', the 121 instances were predicted correctly as class 3, which is keypress '1' action. The best hyperparameters for the model development are tabulated in table 14.

**Table 14.** Best hyperparameters for hybrid Bi-Directional LSTM GRU model

Hyperparameter	Value
Number of LSTM units	128
Number of GRU units	128
Dropout rate	0.2
L2 regularization	0.01
Optimizer	Adam
Loss function	Sparse Categorical Crossentropy
Metrics	Accuracy
Number of epochs	100
Batch size	128
Validation split	0.2
Patience for early stopping	15

### MLP model Results

Finally, MLP model was evaluated with 30% split from total set in order to evaluate the model performance with in-depth analysis. The results from the MLP model yielded that on training an accuracy of 98% can be achieved and on testing 89% accuracy can be achieved with similar result on mean accuracy after 10-fold stratified cross validation.

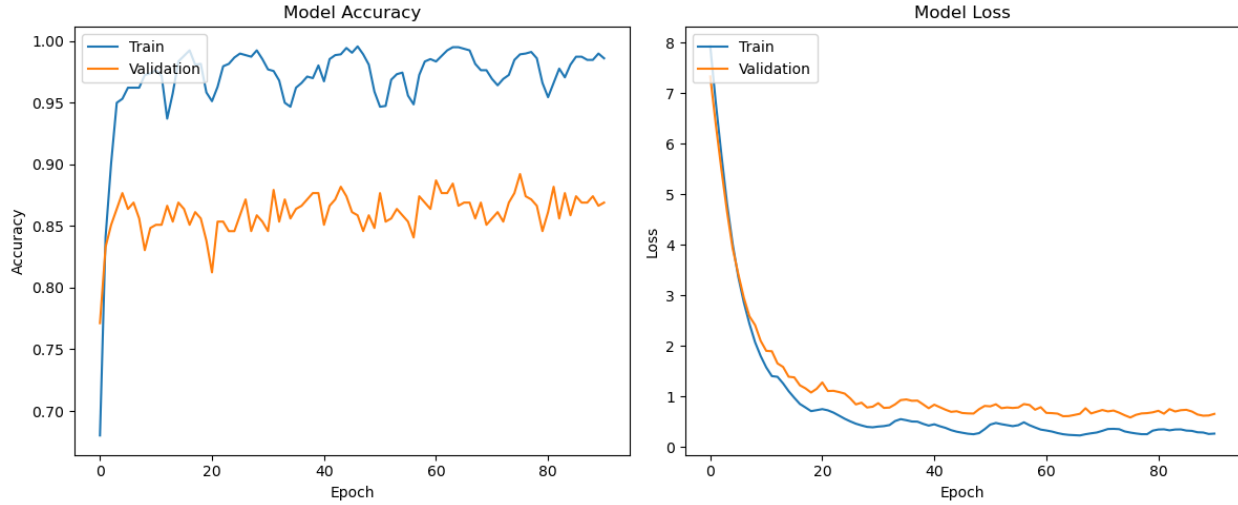


**Fig 22.** Model history plots for MLP model

The approximately 98% training accuracy and the constantly low training loss show that the model has performed well, fitting the training data almost perfectly. The validation performance, however, presents a different picture. Despite initially increasing, the validation accuracy 89% and varies slightly between epochs as seen in figure 22. The model didn't show overfitting and got a validation loss that exhibits instability and levels out higher than the training loss. It does remarkably well on the training set, but as evidenced by the less steady and lower validation accuracy and larger loss, it has trouble generalizing to new data. To improve the model and solve the overfitting problem, regularization approaches, dropout, or early stopping could be used. The mean accuracy on cross validation was 89% with standard deviation of 0.02 which shows the very good performance of model for classifying EEG-based actions.

**Table 15.** Model performance results on each folds

<b>Fold</b>	<b>Testing Accuracy</b>
1	0.87
2	0.88
3	0.88
4	0.86
5	0.91
6	0.88
7	0.92
8	0.89
9	0.87
10	0.89
<b>Mean</b>	<b>0.89</b>
<b>Standard Deviation</b>	<b>0.02</b>

Confusion matrix:



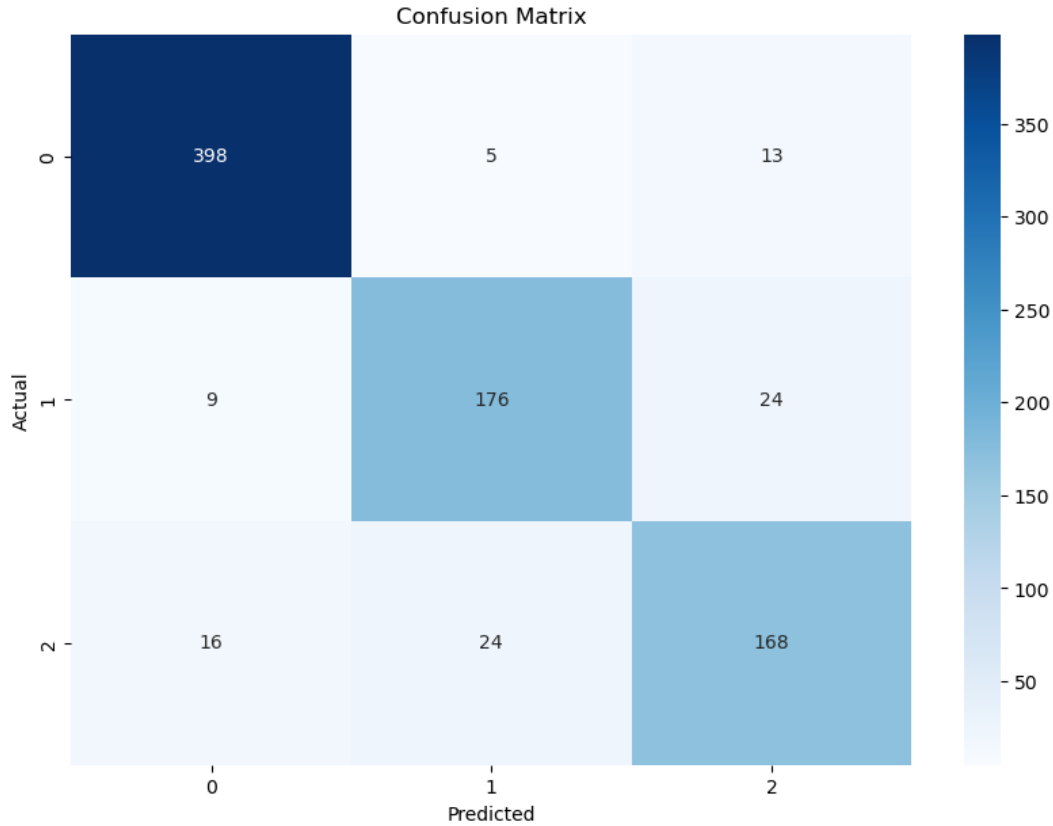


**Fig 23.** Confusion matrix plot for MLP algorithm

The confusion matrix plot for hybrid MLP model on 30% testing set data is shown in figure 23. The confusion matrix plot as shown in figure shows the very good results with 398 instances out of 416 total were predicted correctly for class ‘0’ that is rest state, similarly, out of total 209 instances 176 were predicted correctly as class 1 that is keypress ‘d’ action and finally, out of total 208 instances for class ‘2’ the 168 instances were predicted correctly as class 3 which is keypress ‘1’ action. The hyperparameters for model are tabulated in table 16.

**Table 16.** Tabulated summary of the MLP hyperparameters:

Hyperparameter	Value/Configuration
<b>Standardization</b>	StandardScaler
<b>Model Architecture</b>	Sequential
<b>Layer 1</b>	Dense (256 units, ReLU activation, L2 regularization with 0.01)
<b>Dropout 1</b>	0.2
<b>Layer 2</b>	Dense (128 units, ReLU activation, L2 regularization with 0.01)
<b>Dropout 2</b>	0.2
<b>Layer 3</b>	Dense (64 units, ReLU activation, L2 regularization with 0.01)
<b>Dropout 3</b>	0.2
<b>Output Layer</b>	Dense (softmax activation, units equal to number of unique classes in y)
<b>Optimizer</b>	Adam
<b>Loss Function</b>	Sparse Categorical Crossentropy
<b>Metrics</b>	Accuracy
<b>Batch Size</b>	128
<b>Epochs</b>	100
<b>Validation Split</b>	20% of training data
<b>Early Stopping</b>	Monitor: val_loss, Patience: 15, Restore Best Weights: True

**Table 17.** Overall model classification report comparison

Model	Class	Precision	Recall	F1-Score	Support
MLP	0	0.94	0.96	0.95	416
	1	0.86	0.84	0.85	209
	2	0.82	0.81	0.81	208
MLP Accuracy				0.89	833
MLP Macro Avg		0.87	0.87	0.87	833
MLP Weighted Avg		0.89	0.89	0.89	833
Gaussian NB	0	0.86	0.80	0.87	278
	1	0.70	0.71	0.71	139
	2	0.64	0.57	0.60	139
Gaussian NB Accuracy				0.77	556
Gaussian NB Macro Avg		0.74	0.74	0.74	556
Gaussian NB Weighted Avg		0.77	0.77	0.77	556
KNN	0	0.75	0.95	0.84	268
	1	0.63	0.52	0.57	150
	2	0.59	0.40	0.47	138
KNN Accuracy				0.70	556
KNN Macro Avg		0.66	0.62	0.63	556
KNN Weighted Avg		0.68	0.70	0.68	556
Logistic Regression	0	0.97	0.92	0.94	278
	1	0.87	0.96	0.87	142
	2	0.80	0.87	0.83	136
Logistic Regression Accuracy				0.89	556
Logistic Regression Macro Avg		0.90	0.90	0.90	556
Logistic Regression Weighted Avg		0.91	0.91	0.91	556
Catboost model	0	0.92	0.97	0.94	278
	1	0.83	0.81	0.82	139
	2	0.86	0.78	0.82	139
Catboost Accuracy				0.88	556
Catboost Macro Avg		0.87	0.85	0.86	556
Catboost Weighted Avg		0.88	0.88	0.88	556
SVM Weighted Avg		0.90	0.90	0.90	556
Bi-Directional LSTM-GRU	0	0.95	0.95	0.95	278
	1	0.90	0.80	0.85	139
	2	0.78	0.87	0.82	139
Bi-Directional LSTM-GRU Accuracy				0.89	556
Bi-Directional LSTM-GRU Macro Avg		0.88	0.87	0.87	556
Bi-Directional LSTM-GRU Weighted Avg		0.89	0.89	0.89	556

As shown in table 17. the overall accuracies comparison shows SVM model showing best performance out of all along with Logistic Regression algorithm. To evaluate the performance metrics of different machine learning models, such as MLP, Gaussian NB, KNN, Logistic Regression, SVM, and bi-directional LSTM-GRU, the classification results have been tabulated. For every model, the metrics consist of precision, recall, F1-score, and support for three classes (0, 1, 2). With an overall accuracy of 89% and good F1-scores in every class, the MLP model performs admirably. Both the KNN and Gaussian NB models perform moderately, with accuracies of 78% and comparatively lower F1-scores, especially for class 2. A balanced performance is demonstrated by logistic regression, which has an accuracy of 89% and good precision, recall, and F1-scores, particularly for class 0.

With respect to class 0, the SVM model performs better than the others in terms of precision, recall, and F1-scores; however, the overall accuracy is not specified. With a consistent high metrics across all classes and an accuracy of 89%, the bi-directional LSTM-GRU model also performs well. Based on the available metrics, SVM and Logistic Regression seem to be the most successful models overall, but Gaussian NB and KNN didn't perform much good. The final results obtained can allow us to compare models performances with help of table 18.

**Table 18.** Models obtained mean cross validation accuracies

Model	Accuracy
MLP (Multi-Layer Perceptron)	89%
CatBoost	87.39%
KNN (K-Nearest Neighbors)	72.59%
Gaussian Naive Bayes	79.21%
Logistic Regression	90.81%
SVM	90.42%
Bi-Directional LSTM-GRU Hybrid Model	89%

Evaluating the performance of various models is essential for assuring reliable and consistent results in the construction of a virtual keyboard that uses EEG data to categorize key press occurrences. With the highest mean accuracy of 90.21% of the models examined, the Support Vector Machine (SVM) model stands out. With a standard deviation (SD) of 1.70 and such high accuracy, the SVM model not only performs well but also demonstrates a respectable degree of consistency between runs. The SVM is a great option for applications where accuracy and dependability are crucial because of its performance.

Additionally performing well, the Multilayer Perceptron (MLP) model achieves a mean accuracy of 89.00%. Compared to the SVM, the MLP model has a lower standard deviation of 0.02, indicating that its predictions are more consistent and dependable. The MLP model is a great option for developing an EEG-based virtual keyboard because of its high accuracy and low variability, especially in situations when reliable performance is essential.

In terms of mean accuracy, the Bi-Directional LSTM-GRU hybrid model achieves 89.00%, which is identical to the MLP. On the other hand, its very low standard deviation of just 0.02 shows that it is nearly consistently consistent throughout several runs. The Bi-Directional LSTM-GRU hybrid model may be very dependable for real-time applications where constant performance is crucial, based on its outstanding reliability. Because of its almost nonexistent variability, it is the best choice in situations where steady and consistent outcomes are needed. In the study, logistic regression performed remarkably well in classifying EEG-based events, with an accuracy of 90%. This outcome emphasizes how well logistic regression works as a method for EEG classification problems. Logistic regression is an older and relatively simple algorithm, but it is well-suited for EEG classification because it can model the linear relationship between input features and binary or multinomial outcomes. In EEG classification, a linear model can often capture the decision boundaries between different brain signal patterns. The excellent accuracy attained in this study demonstrates the ongoing use and effectiveness of logistic regression in EEG-based classification issues, particularly in cases where the data has a complex pattern.

High accuracy and reliability are generally shown by the SVM, Logistic Regression, MLP, and Bi-Directional LSTM-GRU hybrid models, which make them excellent choices for categorizing important press events in the creation of EEG-based virtual keyboards. The exact needs for consistency and dependability in the application would determine which of these models to choose.

### GUI output

A dependable and accurate virtual keyboard system that uses EEG signals to anticipate and simulate voluntary key presses is the anticipated result of this Brain-Computer Interface (BCI) project. Based on deep learning architecture, the machine learning model is trained to categorize EEG data into three groups: "resting stage" (0), "d" key press (1), and "I" key press (2). Key presses can be simulated in real time based on the user's brain activity by integrating the trained model into a tkinter-based graphical user interface. With the help of assistive technology, people with neurodegenerative disabilities will be able to interact with digital platforms more effectively by using a virtual

keyboard that is controlled by their brain signals. An example GUI developed using a trained dummy model is shown in the figure below.

On successful testing with a trained SVM model, our model could predict the EEG signal-based classification and could do keypress-based simulation on the GUI, as shown in the figure 24.

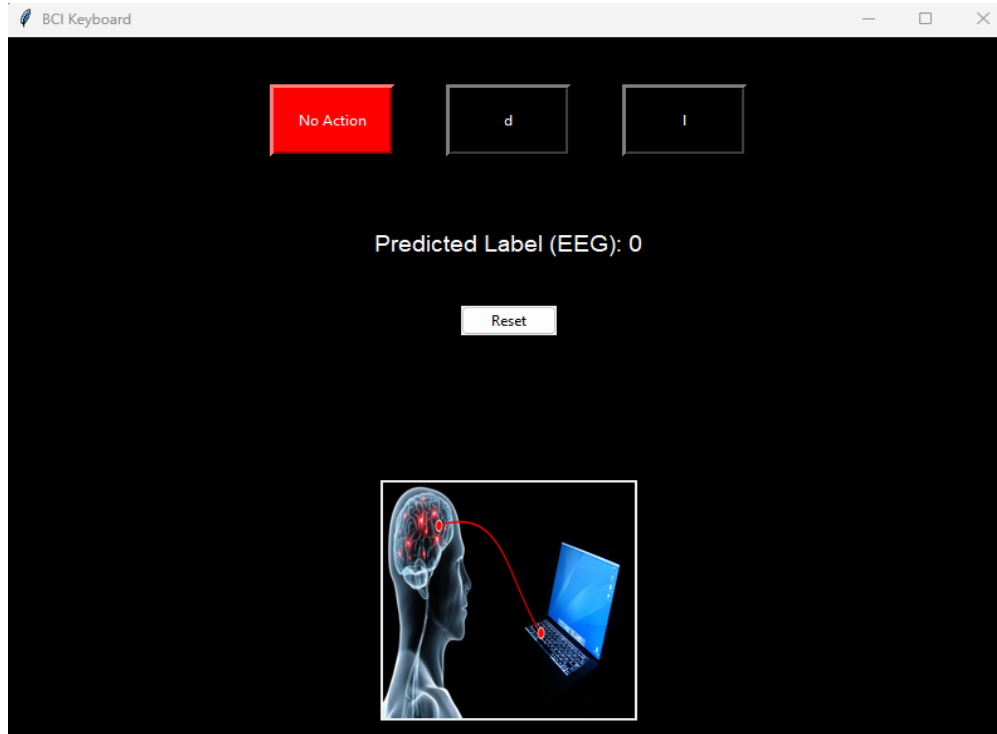


**Fig 24.** Virtual Keyboard GUI

Recent years have witnessed a great deal of progress in the study of brain-machine interfaces, or BMIs [1], [3], [14], [22-25], especially with the development of technologies that connect cerebral activity to mechanical movement. In the beginning, studies concentrated on using electroencephalogram (EEG) signals to operate wheelchairs [17], showcasing the usefulness of non-invasive brainwave monitoring. With this breakthrough, people with physical limitations can now move more freely since it demonstrates how EEG can be used to decipher brain impulses and convert them into controlled movements.

Subsequent to these developments, the area grew even more, encompassing increasingly sophisticated applications like EEG-controlled robotic arms [19]. The hybrid EEG-EOG based keyboards were too developed [7] and users were able to control keyboard with hybrid feature. The successful deployment of these systems demonstrated the EEG-based interfaces' capacity to handle complex tasks and laid the groundwork for investigating even more advanced applications of brainwave data. Notwithstanding these successes, there is still a significant barrier to using EEG for virtual keyboards. The robotic arm-based technologies for lift and grasp tasks are gaining popularity with EEG research [25]. The wheelchair systems based on NeuroSky headsets and eMotiv EPOC Neural Headset [26] with Bluetooth integration [23] have also shown the embedded systems development progress for assistive technology inventions. There is much more need for research on AI technologies like computer vision [22], which has been utilized for ALS patient aid with API-based systems, and similarly, robotic arm control using computer vision has been on research; this can be enhanced with computer vision [24] and EEG integrated systems [14]. Conventional EEG-based virtual keyboards [1], [3], and [15] have had issues with accuracy and user experience because they rely on headsets and EOG signals. Eye blinks-based virtual keyboard were further developed in [30]. [31] but here exists a more need of research in EEG signal utilization for this purpose along with AI integration. These systems frequently suffer from problems including low resolution and signal noise, which can reduce their efficacy and usefulness. EEG

signal processing and use have to be improved due to the limitations of sensor-based systems. The further comparison is made in table 19, which shows previous work methods and results obtained for developing BCI-based systems.

**Table 19.** Comparison with previous works in related areas

<b>Study</b>	<b>Objective</b>	<b>Key Findings</b>	<b>Reference</b>
RSVP Keyboard System	To aid letter selection during brain-typing using RSVP and language models	Accurate letter selection in a single or few trials	[2]
EEG-EOG Hybrid BCI System	Integration of EEG and EOG for virtual keyboard control	EOG traces extracted from EEG signals and treated as an additional input	[3]
EEG-based Game Control	Combining traditional controls with brain signals in games	Identification of attention levels using EEG signals to control 3D environments	[4]
Four States BCI for Neurodegenerative Patients	EEG-based BCI for controlling intelligent devices	Achieved 92.5% average classification accuracy	[5]
Wheelchair Control with Head and Voice Interface	Control of wheelchair using head movements and voice commands	Head control accuracy of 93.3% and 86.6% for two volunteers	[7]
BCI System Using EEG and MPG Signals	EEG and MPG signals used to control a wheelchair via RF	Control based on concentration and eye blinking intensity	[8]
EEG and Microstate Analysis in ALS Patients	EEG spectral band power analysis in ALS patients	Correlation between EEG band power and disease progression	[11]
SSVEP-EOG Hybrid Speller	Integrates SSVEP and EOG for speller system	Average classification accuracy of 94.16%	[12]
Multi-mode EEG Signals Dummy Keyboard	Uses ERP and SSVEP for BCI-based keyboard	SSVEP used for high accuracy in keyboard input	[13]
BCI for ALS Communication via Smartphone	Enable ALS patients to communicate through a smartphone using BCI	Provides a communication interface for ALS patients	[14]
Control Tool using Neurosky Mindwave	Uses frontal lobe signals for PC control via BCI	Achieved typing proficiency with 1.55-1.8 WPM	[15]
EEG-based Wheelchair Control System	Brain-controlled wheelchair using NeuroSky Mindwave	Portable BCI system for wheelchair movement	[18]
Systematic Review of MI-BCI for Wheelchair Control	Overview of MI-BCI applications for wheelchair mobility	Highlights algorithm analysis and classification methods	[19]
Triple RSVP Speller	High ITR and accuracy speller using RSVP	Achieved 0.790 accuracy and 20.259 bit/min ITR	[20]
Brain-Controlled Robotic Arm	Control of a robotic arm using EEG-based BCI	Achieved high accuracy in multi-DoF tasks	[21]
Blink Recognition and User-triggered Actions	Real-time communication via blink detection and actions	Demonstrated accurate blink recognition and timely user actions	[22]
EEG-based Brain-Controlled Wheelchair	Wheelchair controlled by brainwaves using NeuroSky	Movement based on concentration levels and blinks	[23]
Robotic Vision System via GUI	Robotic arm control using a GUI application	Users specify actions via an interactive GUI	[24]

Robotic Arm Control with BCI	Brain-controlled robotic arm with EEG	Successful control of a robotic arm by modulating brain rhythms	[25]
BCI-based Virtual Keyboard with eMotiv EPOC	BCI virtual keyboard for motor-disabled users	Suggested improvements for virtual keyboard effectiveness	[26]
Virtual Keyboard using EEG Signals	QWERTY virtual keyboard with EEG control	Achieved 89.7% accuracy with 6.4 CPM	[27]
This research work	Utilization of machine learning models for making a virtual keyboard based on Right Left-hand voluntary movement and tkinter based virtual keyboard development for classifying 3 actions.	Achieved 89% accuracy on MLP, Bi-Directional LSTM GRU model, and 90% and more accuracy on SVM and logistic regression, along with use of Catboost with 86% accuracy, including KNN and Gaussian NB algorithm. Finally, BCI-based voluntary hand movements-based testing data-based simulating of a virtual TKinter-designed keyboard is possible for predicting 3 actions that include 2 keypresses and a resting state of a person.	

### Future scopes

Our work aims to improve EEG-based virtual keyboards by applying cutting-edge artificial intelligence (AI) techniques in order to overcome these constraints. With the results obtained from this research, our goal is to increase these systems' accuracy and responsiveness by utilizing AI, therefore removing some of the conventional obstacles related to EEG-based interfaces. This strategy not only improves signal processing techniques but also opens up new avenues for more efficient interpretation of brain data. By combining AI with EEG technology, our study fulfills the continuing research requirements and pushes the frontiers of what is feasible in brain-machine communication, thereby representing a significant leap in the field of BMIs [1]. Our research has the potential to significantly impact not only virtual keyboards but also the development of more complex and user-friendly interfaces that may completely change the way people interact with technology through neural signals. In the future, with the trained model BCI, wheelchair-based systems [8], [19], [23] can be developed based on voluntary hand movements, and similarly, other assistive technologies can be developed to pave the path for developing advanced assistive technologies for victims of motor neuron disabilities.

### CONCLUSIONS

The feasibility analysis of the BCI-Based Virtual Keyboard project concludes by highlighting its potential to provide a game-changing solution at the nexus of computing and neuroscience. The technical evaluation showed that training a reliable machine learning model requires a large and representative EEG dataset. Prudent budget allocation for data acquisition, software development, and computational infrastructure is emphasized by financial considerations. In particular for those with neurodegenerative disabilities, operational aspects such as user training and the smooth integration of the model into the GUI are essential to guaranteeing user-friendly interactions.

The need for strict data privacy regulations and adherence to ethical standards in the application of BCI technology is highlighted by legal and ethical feasibility considerations. Successful project execution requires a defined dependencies list, a realistic schedule, and risk mitigation techniques. Market viability illustrates the possible influence of the BCI-based Virtual Keyboard in the assistive technology space by concentrating on user acceptance and competitive positioning. Scalability factors also guarantee adaptability to upcoming technological developments and user needs. Effective risk management is essential to the project's success, especially when it comes to resolving possible problems with data quality and enhancing model performance. The model performance on SVM has shown an exceptional result with nearly 90% accuracy obtained, and validations as well as evaluation metrics also supported model performance.

In conclusion, the thorough feasibility analysis confirms the project's potential to improve accessibility for people with neurodegenerative disabilities and offers a solid basis for the BCI-Based Virtual Keyboard. The project is positioned as a promising endeavor with the potential to make a significant contribution to the field of assistive technology because of its alignment with technical, financial, operational, legal, and ethical considerations as well as its strategic positioning in the market.

## REFERENCES

- [1] Chambayil, B., Singla, R., & Jha, R. (2010). Virtual keyboard BCI using Eye blinks in EEG. In 2010 IEEE 6th International Conference on Wireless and Mobile Computing, Networking and Communications (pp. 466-470). Niagara Falls, ON, Canada. <https://doi.org/10.1109/WIMOB.2010.5645025>.
- [2] Orhan, U., Hild, K. E. II, Erdogmus, D., Roark, B., Oken, B., & Fried-Oken, M. (2012). RSVP Keyboard: An EEG Based Typing Interface. In Proceedings of the IEEE International Conference on Acoustics, Speech, and Signal Processing (ICASSP). <https://doi.org/10.1109/ICASSP.2012.6287966>.
- [3] Hosni, S., Shedeed, H., Mabrouk, M., & Tolba, M. (2019). EEG-EOG based Virtual Keyboard: Toward Hybrid Brain Computer Interface. *Neuroinformatics*, 17, 323-341. <https://doi.org/10.1007/s12021-018-9402-0>.
- [4] Khong, L., Thomas, K. P., & Vinod, A. P. (2014). BCI based multi-player 3-D game control using EEG for enhancing attention and memory. In 2014 IEEE International Conference on Systems, Man, and Cybernetics (SMC) (pp. 1847-1852). San Diego, CA, USA. <https://doi.org/10.1109/SMC.2014.6974189>.
- [5] Junwei, L., et al. (2019). Brain Computer Interface for Neurodegenerative Person Using Electroencephalogram. *IEEE Access*, 7, 2439-2452. <https://doi.org/10.1109/ACCESS.2018.2886708>.
- [6] Kaya, M., Binli, M., Ozbay, E., et al. (2018). A large electroencephalographic motor imagery dataset for electroencephalographic brain computer interfaces. *Sci Data*, 5, 180211. <https://doi.org/10.1038/sdata.2018.211>.
- [7] Hosni, S. M., Shedeed, H. A., Mabrouk, M. S., & Tolba, M. F. (2019). EEG-EOG based Virtual Keyboard: Toward Hybrid Brain Computer Interface. *Neuroinformatics*, 17(3), 323-341. <https://doi.org/10.1007/s12021-018-9402-0>.
- [8] Altorabi, H., & Al-Junaid, H. (2018). Brain Computer Interface for Wheelchair Control in Smart Environment. In Proceedings of the 23rd International Conference on Automation and Computing (pp. 23 (6 pp.)-23 (6 pp.)). <https://doi.org/10.1049/cp.2018.1391>.
- [9] Chaddad, A., Wu, Y., Kateb, R., & Bouridane, A. (2023). Electroencephalography Signal Processing: A Comprehensive Review and Analysis of Methods and Techniques. *Sensors (Basel)*, 23(14), 6434. <https://doi.org/10.3390/s23146434>.
- [10] Rayi, A., & Murr, N. (2024). Electroencephalogram. In StatPearls [Internet]. Treasure Island (FL): StatPearls Publishing. Available from: <https://www.ncbi.nlm.nih.gov/books/NBK563295>.
- [11] Notturmo, F., Croce, P., Ornello, R., Sacco, S., & Zappasodi, F. (2023). Yield of EEG features as markers of disease severity in amyotrophic lateral sclerosis: a pilot study. *Amyotrophic Lateral Sclerosis and Frontotemporal Degeneration*, 24(3-4), 295-303. <https://doi.org/10.1080/21678421.2022.2152696>.



- [12] Saravanakumar, D., & Reddy, M. R. (2020). A virtual speller system using SSVEP and electrooculogram. *Advanced Engineering Informatics*, 44, 101059. <https://doi.org/10.1016/j.aei.2020.101059>.
- [13] Xu, X., & Ding, R. (2018). A kind of EEG signals dummy keyboard design method based on multi-mode (CN108681391A). Nanjing University of Posts and Telecommunications.
- [14] Mir, N., Sarirete, A., Hejres, J., & Al Omairi, M. (2019). Use of EEG Technology with Based Brain-Computer Interface to Address Amyotrophic Lateral Sclerosis—ALS. In Visvizi, A., Lytras, M. (eds), *Research & Innovation Forum 2019. RIIFORUM 2019. Springer Proceedings in Complexity*. Springer, Cham. [https://doi.org/10.1007/978-3-030-30809-4\\_39](https://doi.org/10.1007/978-3-030-30809-4_39).
- [15] Salih, T. A., & Abdal, Y. M. (2020). Brain computer interface based smart keyboard using neurosky mindwave headset. *TELKOMNIKA Telecommunication, Computing, Electronics and Control*, 18(2), 919-927. <https://doi.org/10.12928/TELKOMNIKA.v18i2.13993>.
- [16] Fraschini, M., Demuru, M., Hillebrand, A., et al. (2016). EEG functional network topology is associated with disability in patients with amyotrophic lateral sclerosis. *Sci Rep*, 6, 38653. <https://doi.org/10.1038/srep38653>.
- [17] Karikari, E., & Koshechkin, K. A. (2023). Review on brain-computer interface technologies in healthcare. *Biophys Rev*, 15(5), 1351-1358. <https://doi.org/10.1007/s12551-023-01138-6>.
- [18] Sharma, H., et al. (2021). Conference Paper Title. *Journal of Physics: Conference Series*, 1969, 012065. <https://doi.org/10.1088/1742-6596/1969/1/012065>.
- [19] Palumbo, A., Gramigna, V., Calabrese, B., & Ielpo, N. (2021). Motor-Imagery EEG-Based BCIs in Wheelchair Movement and Control: A Systematic Literature Review. *Sensors (Basel)*, 21(18), 6285. <https://doi.org/10.3390/s21186285>.
- [20] Lin, Z., Zhang, C., Zeng, Y., et al. (2018). A novel P300 BCI speller based on the Triple RSVP paradigm. *Sci Rep*, 8, 3350. <https://doi.org/10.1038/s41598-018-21717-y>.
- [21] Meng, J., Zhang, S., Bekyo, A., et al. (2016). Noninvasive Electroencephalogram Based Control of a Robotic Arm for Reach and Grasp Tasks. *Sci Rep*, 6, 38565. <https://doi.org/10.1038/srep38565>.
- [22] Paneru, B., & Paneru, B. (2023). Computer Vision in Healthcare: ALS Patient Aid Application with Computer Vision & Green API. Available at SSRN: <https://ssrn.com/abstract=4918906>.
- [23] Dev, A., Rahman, M. A., & Mamun, N. (2018). Design of an EEG-Based Brain Controlled Wheelchair for Quadriplegic Patients. In *Proceedings of the IEEE International Conference on Communication and Technology (I2CT)* (pp. 1-5). <https://doi.org/10.1109/I2CT.2018.8529751>.

- [24] Intisar, M., Khan, M., Islam, M., & Masud, M. (2021). Computer Vision Based Robotic Arm Controlled Using Interactive GUI. *Intelligent Automation & Soft Computing*, 27, 533-550. <https://doi.org/10.32604/iasc.2021.015482>.
- [25] Meng, J., Zhang, S., Bekyo, A., Olsoe, J., Baxter, B., & He, B. (2016). Noninvasive Electroencephalogram Based Control of a Robotic Arm for Reach and Grasp Tasks. *Sci Rep*, 6, 38565. <https://doi.org/10.1038/srep38565>. Erratum in: *Sci Rep*, 10(1), 6627. <https://doi.org/10.1038/s41598-020-63070-z>.
- [26] Corley, J., Heaton, D., Gray, J., Carver, J., & Smith, R. (2012). Brain-Computer Interface Virtual Keyboard for Accessibility. *Computers and their Applications*, 10.2316/P.2012.772-036.
- [27] Reddy, S., Jagtap, P., Jagtap, S., & Ghodke, A. (2023). RGB Based EEG Controlled Virtual Keyboard & Mouse for Physically Challenged People. *International Research Journal of Modernization in Engineering, Technology and Science*, 5(5).
- [28] N. Naseeb, M. Alam, O. B. Samin, M. Omar, S. S. Khushbakht and S. A. Shah, "RGB based EEG Controlled Virtual Keyboard for Physically Challenged People," *2020 3rd International Conference on Computing, Mathematics and Engineering Technologies (iCoMET)*, Sukkur, Pakistan, 2020, pp. 1-5, doi: 10.1109/iCoMET48670.2020.9073847.
- [29] R. Scherer, G. R. Muller, C. Neuper, B. Graimann and G. Pfurtscheller, "An asynchronously controlled EEG-based virtual keyboard: improvement of the spelling rate," in *IEEE Transactions on Biomedical Engineering*, vol. 51, no. 6, pp. 979-984, June 2004, doi: 10.1109/TBME.2004.827062.
- [30] Rusanu, O. A., Cristea, L., Luculescu, M. C., Cotfas, P. A., & Cotfas, D. T. (2019). Virtual Keyboard Based on a Brain-Computer Interface. *IOP Conference Series: Materials Science and Engineering*, 514(1), 012020. <https://doi.org/10.1088/1757-899X/514/1/012020>

•